



# **Earth Model Selection for Computer Simulations**

**J. J. PICH AND S. S. LEROY**

*ENEWS Program  
Tactical Electronic Warfare Division*

**December 15, 1989**

REPORT DOCUMENTATION PAGE			Form Approved OMB No. 0704-0188	
Public reporting burden for this collection of information is estimated to average 1 hour per response, including the time for reviewing instructions, searching existing data sources, gathering and maintaining the data needed, and completing and reviewing the collection of information. Send comments regarding this burden estimate or any other aspect of this collection of information, including suggestions for reducing this burden, to Washington Headquarters Services, Directorate for Information Operations and Reports, 1215 Jefferson Davis Highway, Suite 1204, Arlington, VA 22202-4302, and to the Office of Management and Budget, Paperwork Reduction Project (0704-0188), Washington, DC 20503.				
1. AGENCY USE ONLY (Leave blank)	2. REPORT DATE December 15, 1989	3. REPORT TYPE AND DATES COVERED Final		
4. TITLE AND SUBTITLE  Earth Model Selection for Computer Simulations		5. FUNDING NUMBERS  PE-64255N PR-X0672 WU-DN120-188		
6. AUTHOR(S)  Pich, J. J. and Leroy, S. S.				
7. PERFORMING ORGANIZATION NAME(S) AND ADDRESS(ES)  Naval Research Laboratory Washington, DC 20375-5000		8. PERFORMING ORGANIZATION REPORT NUMBER  NRL Report 9227		
9. SPONSORING/MONITORING AGENCY NAME(S) AND ADDRESS(ES)  Naval Air Systems Command Washington, DC 20361		10. SPONSORING/MONITORING AGENCY REPORT NUMBER		
11. SUPPLEMENTARY NOTES				
12a. DISTRIBUTION / AVAILABILITY STATEMENT  Approved for public release; distribution unlimited.		12b. DISTRIBUTION CODE		
13. ABSTRACT (Maximum 200 words)  Many scientific problems require the use of appropriate Earth models. This report presents a method of selecting from a variety of these models on the basis of range and bearing errors and CPU timing considerations that are incurred by each.  The report begins by examining two types of flat Earth models and determines the better of the two. The reference for the determinations of all errors is the DoD standard Earth model representation, the World Geodetic System (WGS-84) reference ellipsoid. The report shows that for short distances a "Midpoint Flat Earth" model is adequate at low latitudes. However, for longer ranges, better Earth models must be employed. The report proceeds to compare five spherical Earth models (different radii based on different assumptions). A model referred to as the "Spherical Approximation" is shown to be a superior representation that allows for an increase in the permissible distance coverage under various constraining error budgets. For an error budget of 1000 m, the representation can be used to compute distances up to 250 nmi in the midlatitudinal region of 40°N to 70°N. For distances beyond 250 nmi, only a WGS-84 reference ellipsoid representation is adequate for the 1000-m error budget.				
14. SUBJECT TERMS		15. NUMBER OF PAGES 53		16. PRICE CODE
17. SECURITY CLASSIFICATION OF REPORT UNCLASSIFIED	18. SECURITY CLASSIFICATION OF THIS PAGE UNCLASSIFIED	19. SECURITY CLASSIFICATION OF ABSTRACT UNCLASSIFIED	20. LIMITATION OF ABSTRACT SAR	

## CONTENTS

INTRODUCTION .....	1
FLAT EARTH MODELS .....	1
SPHERICAL EARTH MODELS .....	3
ELLIPSOID EARTH MODELS .....	4
ANALYSIS .....	4
Range and Bearing Errors .....	4
Flat Earth Models .....	5
Spherical Earth Models .....	7
Comparison of Flat Earth and Spherical Earth Models .....	7
Comparison of Spherical Approximation Model and WGS-84 Ellipsoidal Model .....	11
Timing Considerations .....	12
Summary .....	17
APPLICATION TO ENEWS SIMULATIONS .....	17
CONCLUSIONS .....	19
RECOMMENDATIONS .....	20
ACKNOWLEDGMENTS .....	20
REFERENCES .....	20
APPENDIX A — The Geodetic Inverse Solution Subroutine .....	21
APPENDIX B — The Geodetic Direct Solution Subroutine .....	25
APPENDIX C — Chordal Distance Calculation Subroutine .....	29
APPENDIX D — Flat Earth Model Analysis .....	31
APPENDIX E — Spherical Earth Model Analysis .....	35
APPENDIX F — Comparisons of Flat Earth Models To Spherical Approximation Model .....	43

# **EARTH MODEL SELECTION FOR COMPUTER SIMULATIONS**

## **INTRODUCTION**

The Effectiveness of Navy Electronic Warfare Systems (ENEWS) Program in the Tactical Electronic Warfare Division (TEWD) of the Naval Research Laboratory (NRL) came into being in 1971 to provide the electronic warfare (EW) community the analytical tools with which to perform EW system performance assessments. To satisfy this need, ENEWS has generated a wide variety of computational tools, and, from the beginning, has used digital computers to create simulated electromagnetic (EM) environments (scenarios). These environments include motion for subsurface, surface, and airborne elements of tactical engagements, and the necessary parameters for generating signal emissions. Until the early 1980s, these tactical situations covered distances of not more than 100 to 200 nmi and were placed in open ocean and midlatitudinal regions. A flat Earth model representation has served adequately for such scenarios. However, over the last 6 to 10 years, mission requirements had to include Earth satellites, sea launched ballistic missiles (SLBM), sea launched cruise missiles (SLCM), and hostile long-range bombers and reconnaissance aircraft. All these elements can operate over greater distances than 200 nmi as well as at high latitudes and hence require the use of Earth models that remain accurate within tolerance over long distances. This report provides a basis for selecting an appropriate Earth model that will allow for the inclusion of the elements already mentioned and that can solve future problems.

The selection of an appropriate Earth model is one of the first tasks that analysts perform to construct computer simulations requiring range and bearing computations. Frequently, a selection is made solely on the basis of ease of implementation. This approach may yield adequate results under certain conditions and error tolerances as indicated above in the ENEWS experience. However, as demonstrated in this report, the selection of a particular Earth model may not necessarily yield the best approach. For example, the choice of one Earth model applied at equatorial regions may not remain within the required error budget when it is applied at midlatitudinal regions. In fact, to remain within certain accuracies, it may be required to use several Earth models selectively depending upon location and distances within the same application program. The prime intent of this analysis is to provide a method for selecting an appropriate Earth model based on allowable range errors and CPU timing. The analysis summary provides a useful nomogram for performing this function.

Specifically, this report is a study of three different categories of Earth models; flat Earth, spherical Earth, and ellipsoidal Earth. Within each category, two or more approaches are examined to determine whether any significant differences exist within the category. CPU utilization analyses are performed and included for completeness.

## **FLAT EARTH MODELS**

A typical flat Earth model uses a transformation that is valid for small areas of coverage. Because of its simplicity, it is computed very fast. This transformation assumes that the Earth is spherical with a

circumference of 21,600 nmi and that corresponds to a distance of 60 nmi/deg along any great circle. For reference purposes throughout this report, the sphere is referred to as the Navigation Sphere. When site locations are given as latitudes and longitudes, the positions are converted to a flat Earth approximation by using these criteria. Details of this transformation are summarized here for ready reference.

The transformation from the Navigation Sphere to the flat Earth approximation is established by taking two Points,  $O$  and  $A$ , on the surface of this sphere. These points are defined by geodetic coordinates  $(\phi_1, \lambda_1)$  and  $(\phi_2, \lambda_2)$  respectively, where  $\phi_i$  and  $\lambda_i$  are the latitude and longitude respectively. A mapping of the difference in latitude and longitude onto a flat plane is given by

$$\begin{aligned} \Delta y &= 60 \Delta \phi \\ \Delta x &= 60 \Delta \lambda \cos \phi_2 \end{aligned} \tag{1}$$

where

$$\begin{aligned} \Delta \phi &= \phi_2 - \phi_1 \\ \Delta \lambda &= \lambda_2 - \lambda_1 \end{aligned}$$

and where the measurement is made from point  $O$  (the observer) to Point  $A$ . By using this transformation, for point  $O$  on the plane  $(x_1, y_1)$  and differences in latitude and longitude  $\Delta \phi$ ,  $\Delta \lambda$ , the terminal point  $A$   $(x_2, y_2)$  computes as follows:

$$\begin{aligned} y_2 &= y_1 + \Delta y \\ x_2 &= x_1 + \Delta x \end{aligned} \tag{2}$$

where  $\Delta y$  and  $\Delta x$  are given by Eq. (1).

Figure 1 shows this transformation, where point  $O$  is the observation point and point  $A$  on the sphere is mapped (by Eq. (2)) to point  $A'$  on the  $x, y$  plane. Figure 2 shows the associated bearing relationships. In both figures the point of tangency is assumed to be at point  $O$ . From the preceding formulas, the distance  $OA'$  is calculated as shown in Eq. (3):

$$OA' = \sqrt{\Delta x^2 + \Delta y^2} \tag{3}$$

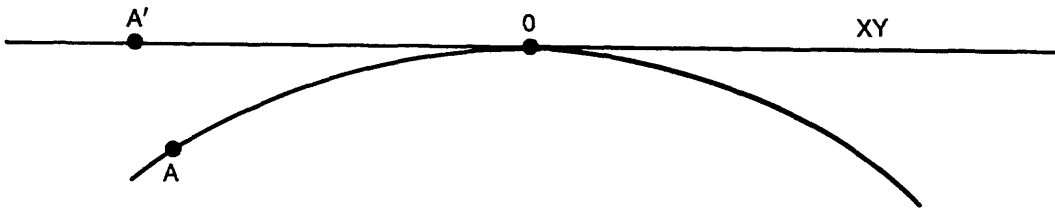


Fig. 1 — Distance relationship of XY flat Earth and reference ellipsoid

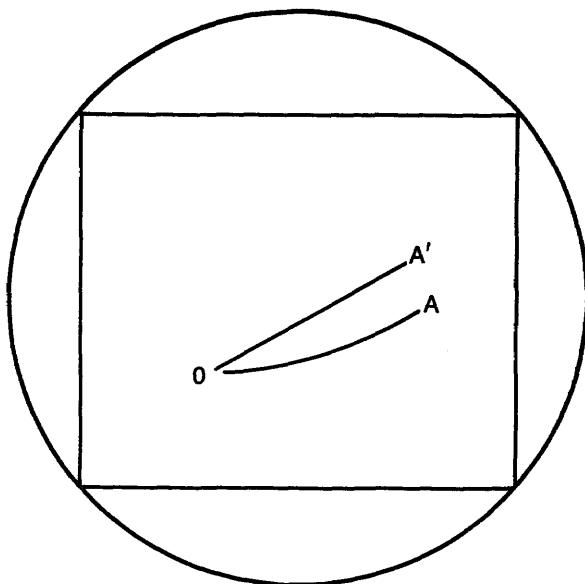


Fig. 2 — Bearing relationship of XY flat Earth and reference ellipsoid

Equation (1) uses the cosine of the latitude  $\phi_2$  at Point  $A$  to modify the longitudinal difference,  $\Delta\lambda$ . For minor latitude differences (small  $\Delta\phi$ ) with point  $O$  at or near the equator, this calculation may be satisfactory. A more precise calculation can be obtained by taking the cosine of the mean latitude. Thus,  $\Delta x$  in Eq. (1) becomes:

$$\Delta x = 60 \Delta\lambda \cos \left[ \frac{\phi_1 + \phi_2}{2} \right]. \tag{4}$$

This technique provides a negligible difference in computer run time when compared to the first method, and it is considered to be more accurate. For reference, Eq. (1) will be called the End Point Flat Earth model, and Eq. (4) and  $\Delta y$  from Eq. (1) will be called the Midpoint Flat Earth model.

### SPHERICAL EARTH MODELS

To obtain the simplest progression from a flat Earth model, a spherical Earth model is used. In geodetic computations, several spheres are commonly used

- |                            |                        |
|----------------------------|------------------------|
| 1. Mean-Axis Sphere        | radius = 6370291.091 m |
| 2. Equal-Surface Sphere    | radius = 6370289.510 m |
| 3. Equal-Volume Sphere     | radius = 6370283.158 m |
| 4. Navigation Sphere       | radius = 6366707.019 m |
| 5. Spherical Approximation | radius = 6371000.000 m |

The first three spheres are discussed in Ref. 1. As previously mentioned, the Navigation Sphere corresponds to a sphere of 60 nmi/deg on any great circle. Finally, for the Earth's spherical radius a rounded-off number of 6,371,000 m is sometimes used to solve geodetic problems. Throughout this report, this sphere is referred to as the "Spherical Approximation."

## ELLIPSOID EARTH MODELS

The geometric representation of the Earth with geodetic accuracy is obtained by using a rotational ellipsoidal model. This is possible because of the ever-improving ground and satellite sensors that provide more accurate positional and gravitational data that, in turn, yield improved values of associated reference ellipsoid constants. A rotational ellipsoid is defined by two constants, the semimajor axis  $a$  (Earth's radius at the equator), and the semiminor axis  $b$  (Earth's radius at the poles). An alternative constant, mathematically related to the axes [2], is called the flattening  $f$  given by

$$f = \frac{a - b}{a},$$

where

- $f$  is the flattening,
- $a$  is the semimajor (equatorial) axis, and
- $b$  is the semiminor (polar) axis.

The ellipsoid is normally specified by giving  $a$  and  $f$ ;  $b$  is then readily calculated by solving for  $b$  in the equation:

$$b = a(1 - f).$$

For many Earth models, this flattening is approximately 1/300 [3].

Many ellipsoids have been developed and used for more than a century. Table 1 shows a partial list of such ellipsoids, most of which were designed to be used for specific geographic locations. For the past few decades, attempts have been focused on the development of a generalized ellipsoid model for the entire Earth. The ellipsoid used as a reference for this report is the most recent one defined by the Defense Mapping Agency (DMA); it is called the Department of Defense (DoD) World Geodetic System 1984, or WGS-84. Table 1 shows the primary reference ellipsoid constants that define this ellipsoid. The ellipsoid should provide surface distance measurement accuracies within a few meters anywhere on the Earth. Current geodetic data generated by DMA, including digital terrain elevation data (DTED), are based on the WGS-84 ellipsoid. Reference 2 provides details of the WGS-84 ellipsoid.

Appendixes A and B provide the program code for any ellipsoid defined by the semimajor and semiminor axes. The "Inverse Solution" provides a distance and bearing calculation, given the latitudes and longitudes of two end points. The "Direct Solution" calculates a second point, given the latitude and longitude of an initial point, with the distance and bearing to the end point. The spherical computation is available with either of these solutions, by selecting the semimajor and semiminor axes to be identical ( $a = b$ ).

## ANALYSIS

### Range and Bearing Errors

This analysis determines the limits over which each of the three basic Earth models (flat, spherical, ellipsoidal) can be used. It is important to determine acceptable distance and positional accuracies for simulations that require the use of an Earth model.

The approach uses a computer program that exercises the ellipsoid programs as listed in Appendixes A and B, along with a flat Earth model. This program, computes polar plots of range errors and begins by

Table 1 — Reference Ellipsoid Constants

Reference Ellipsoid	Year	Semimajor axis (m) <i>a</i>	Flattening <i>f</i>	Used in/by
Airy	1830	6377563.396	1/299.3249646	Great Britain
Everest	1830	6377276.345	1/300.8017	India
Hough	1830	6378270	1/297	Wake-Eniwetok
Bessel	1841	6377397.155	1/299.1528128	Japan
Clarke	1866	6378206.4	1/294.9786982	North America
Clarke	1880	6378249.145	1/293.465	France, Africa
International	1924	6378388	1/297	Europe
Krassowsky	1940	6378245	1/298.3	Russia
WGS-60	1960	6378165	1/298.3	
Fischer (Mercury)	1960	6378166	1/298.3	
WGS-66	1966	6378145	1/298.25	DoD Products
GRS 67	1967	6378160	1/298.25	Australia, South America
Fischer	1968	6378150	1/298.3	South Asia
WGS-72	1972	6378135	1/298.26	DoD Products
GRS 80	1979	6378137	1/298.257222101	North America
WGS-84	1985	6378137	1/298.257223563	DoD Products

generating a circle centered on an observation point with a predetermined range. The WGS-84 Direct Solution calculates the latitudes and longitudes of points on that circle, in 1° steps. Then the flat Earth and spherical Earth models are exercised with their associated inverse programs to calculate the distance (range). The calculated ranges are then compared to the predetermined range to obtain a range error. The range error assumes the WGS-84 ellipsoid as a reference. Bearing errors are also calculated by comparing the calculated bearing with the input azimuth angle used to generate the data.

*Flat Earth Models*

The analysis compares the two flat Earth models described earlier. Polar plots of the range and bearing errors have been generated for various ranges. The program steps in preparing the plots are as follows:

1. Select the range at which errors will be calculated.
2. Select the observer latitude and longitude.
3. Loop through 360° in 1° steps.
4. Use the WGS-84 Direct Solution to determine the latitudes and longitudes of points on the range circle in 1° increments.
5. Use the two flat Earth inverse functions to calculate new ranges and bearings, given the latitudes and longitudes from steps 2 and 4.
6. Compare the newly calculated ranges with the selected range from step 1 for range errors.
7. Compare the newly calculated bearings with the azimuths defined in step 3 for bearing errors.

Figures 3 and 4 show the range and bearing errors incurred at 45°N 0°E for a distance of 100 nmi. These and other figures are presented in detailed analyses in Appendix D. Figure 3 shows the improvement gained by using the Midpoint Flat Earth model instead of the End Point Flat Earth model.

PICH AND LEROY

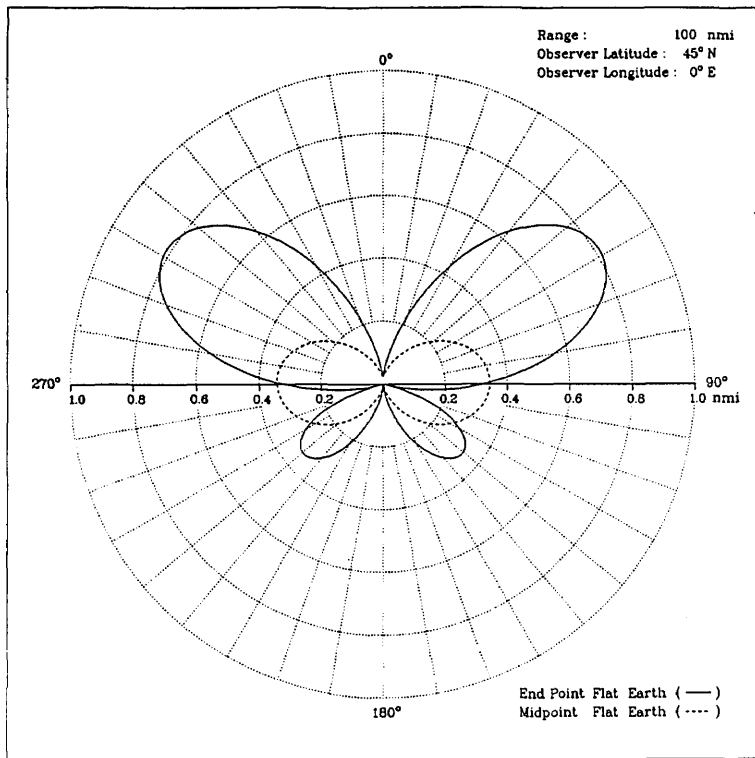


Fig. 3 — Flat Earth range errors vs azimuth

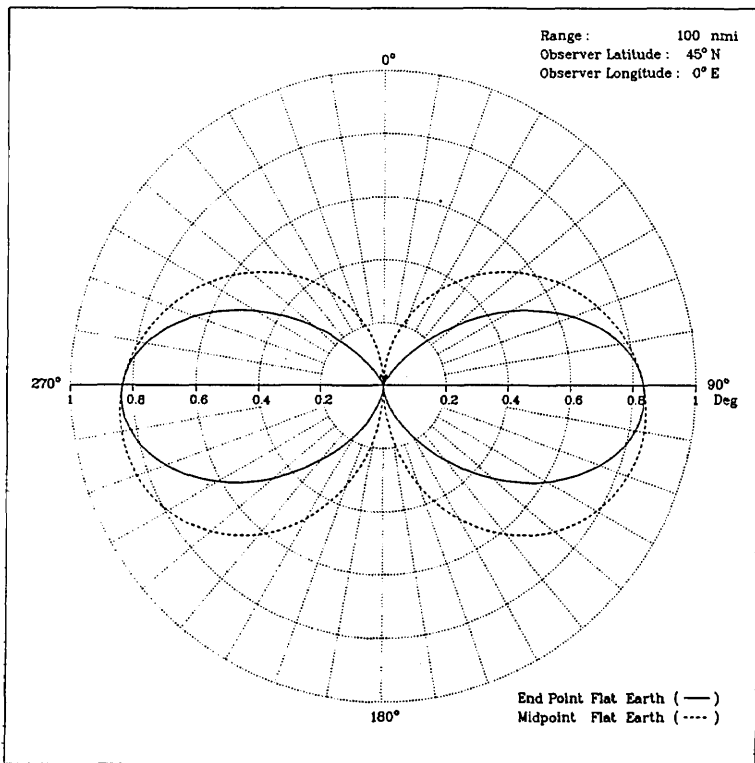


Fig. 4 — Flat Earth bearing errors vs azimuth

*Spherical Earth Models*

The next step is to select an appropriate spherical Earth model. The flat Earth programming steps discussed earlier are used again. Spherical models are substituted in step 5; they are those used in the ellipsoidal solutions of Appendixes A and B, with equal radius values for the semimajor and semiminor axes. The five spheres already described are reduced to three spheres, because the first three in the list are, for practical purposes, indistinguishable. Those chosen for further study are the Equal Volume, the Spherical Approximation, and the Navigation Sphere.

Figure 5 shows a graph of the selected three spherical models at 500 nmi from the observation point 45°N 0°E. At this latitude and distance the Spherical Approximation model is predominantly better than either of the other two spherical Earth models. Appendix E furnishes additional comparisons at different latitudes and ranges.

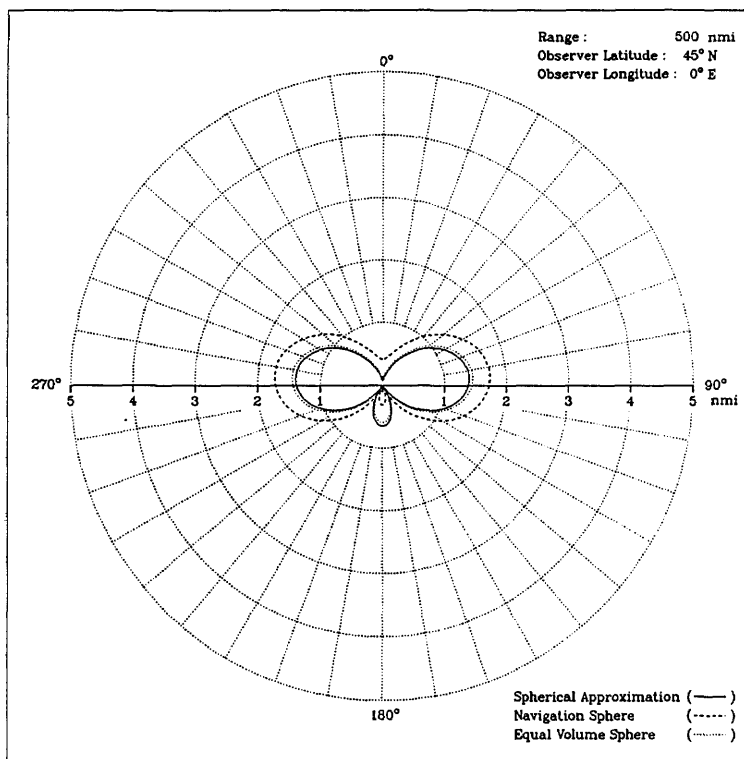


Fig. 5 — Spherical Earth range errors vs azimuth

*Comparison of Flat Earth and Spherical Earth Models*

The analysis now determines the appropriate domains over which flat, spherical, and ellipsoidal Earth models should be used. It is clear, from the preceding analysis, that depending on the application and allowable error tolerances, sufficient choices of models exist that can be used. However, it is more difficult to see when the adequacy of a model stops. This section of the report attempts to focus on this question solely on the basis of range error analyses.

We reexamine the two flat Earth models previously discussed. By generating data as shown in Fig. 3, but for a large number of radial ranges up to 500 nmi, we obtain the maximum range error incurred at each

of the radial distances. Thus, Fig. 6 illustrates the error incurred by the End Point Flat Earth model. Similar calculations are also performed by using the Midpoint Flat Earth and Spherical Approximation models and are placed on the same graph shown in Fig. 6. Appendix F shows similar graphs computed at other latitudes.

The analysis now proceeds to determine the error contours for the Midpoint Flat Earth model as a function of latitude. By generating the same type of data as shown in Fig. 3, but taken at  $1^\circ$  increments of observer latitude, it is possible to determine the range distances for a 1-nmi error, 2-nmi error, etc. This produces the contours that are shown in Figs. 7 through 10. Figure 7 shows the End Point Flat Earth model contours, and Fig. 8 shows the Midpoint Flat Earth model contours. Figures F1 through F7 in Appendix F compare the behavior of the End Point Flat Earth model to the Midpoint Flat Earth model at six selected latitudes. Figures 7 and 8 provide the expansion of these data from the equator to the north polar region. The 1-nmi error contour shows the distance to which one can go to incur not more than a 1-nmi error at any latitude north of the equator. Thus, for example, in Fig. 7, if an observer is at  $40^\circ\text{N}$  and if the distance between the observer and a second point is less than or equal to 125 nmi, distances can be computed accurately to within 1 nmi. Using the Midpoint Flat Earth model (Fig. 8) at the same latitude, the 1-nmi tolerance extends to approximately 360 nmi. A direct comparison of all the contours in Fig. 7 and 8 reveals that the Midpoint Flat Earth model is superior to the End Point Flat Earth model in error tolerance at all latitudes over all surface ranges. It is clear, therefore, that, since the computational requirements for these two models are equivalent (Eqs. (1) and (4)), the Midpoint Flat Earth model is preferable.

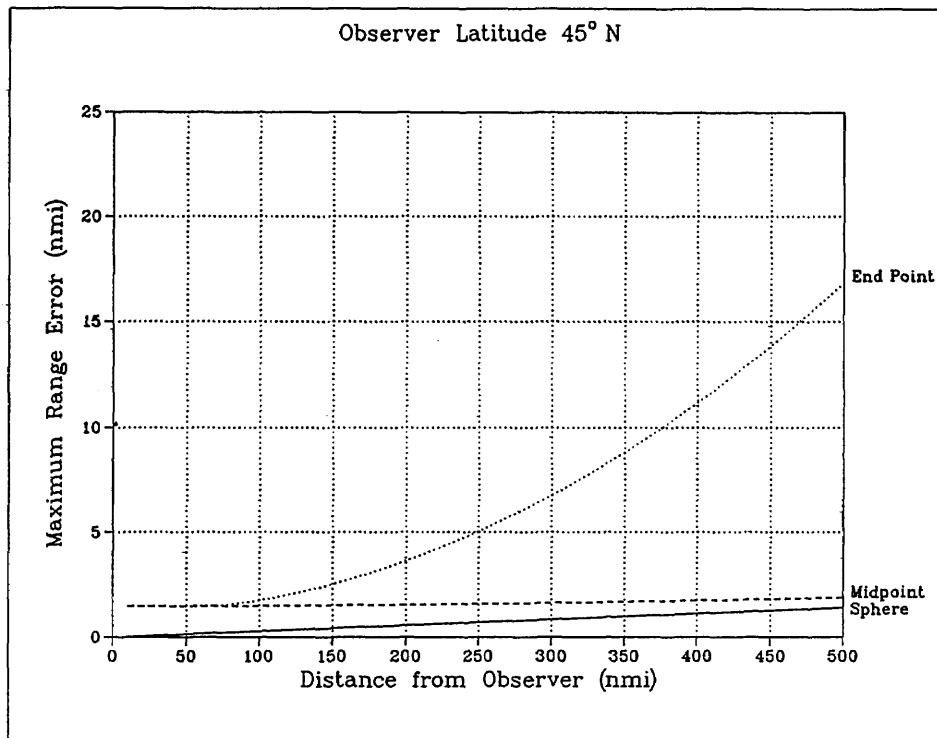


Fig. 6 — Surface range errors vs surface range

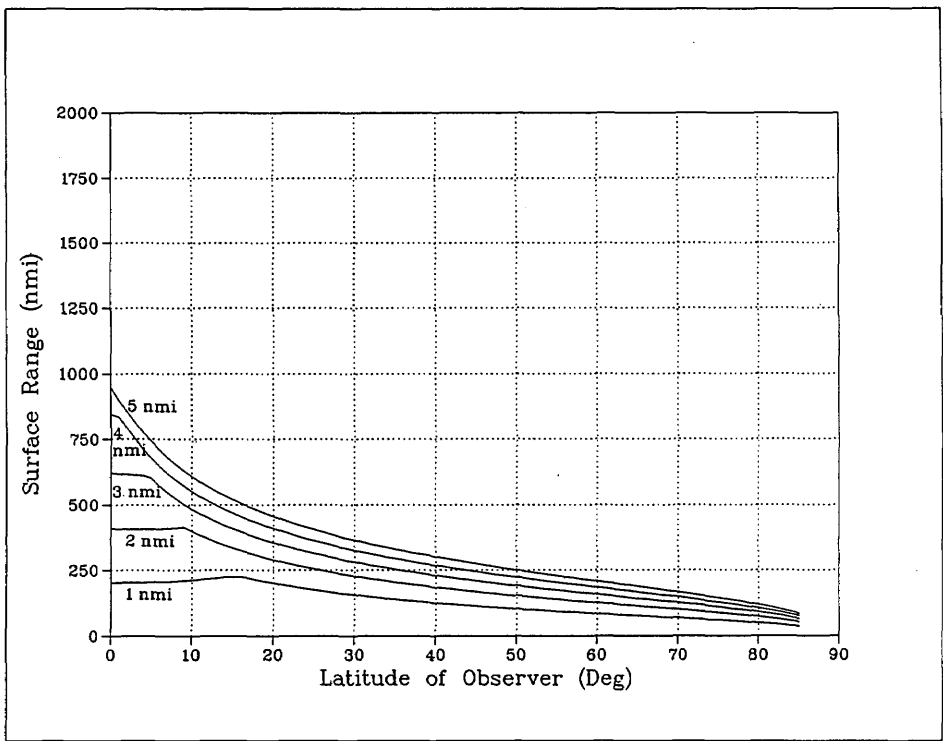


Fig. 7 — End Point Flat Earth range error contours vs observer latitude

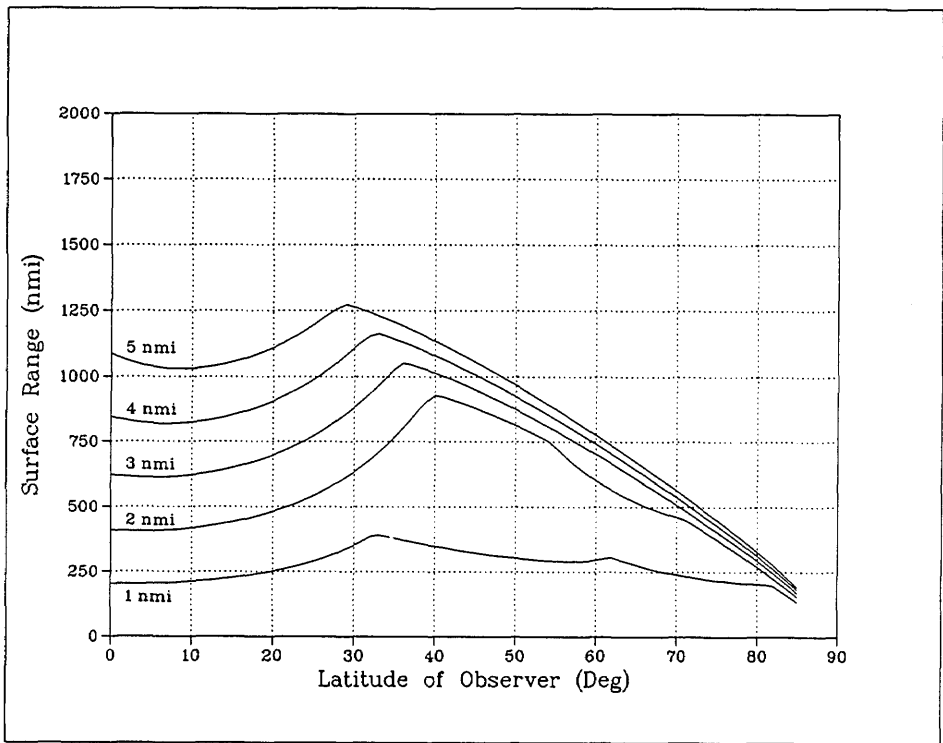


Fig. 8 — Midpoint Flat Earth range error contours vs observer latitude

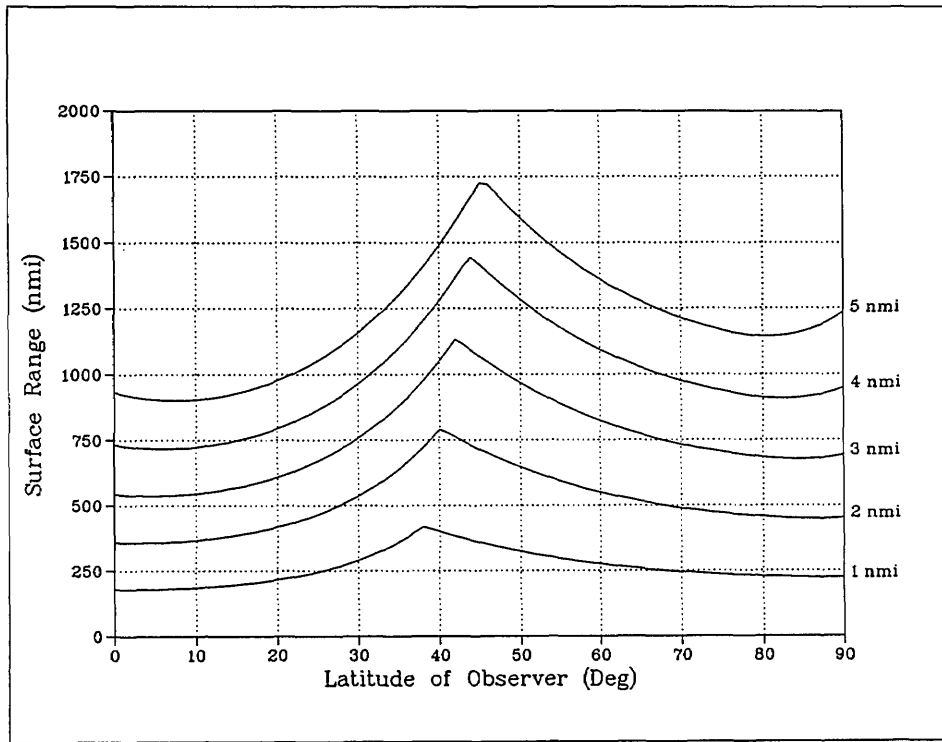


Fig. 9 — Spherical Approximation range error contours vs observer latitude

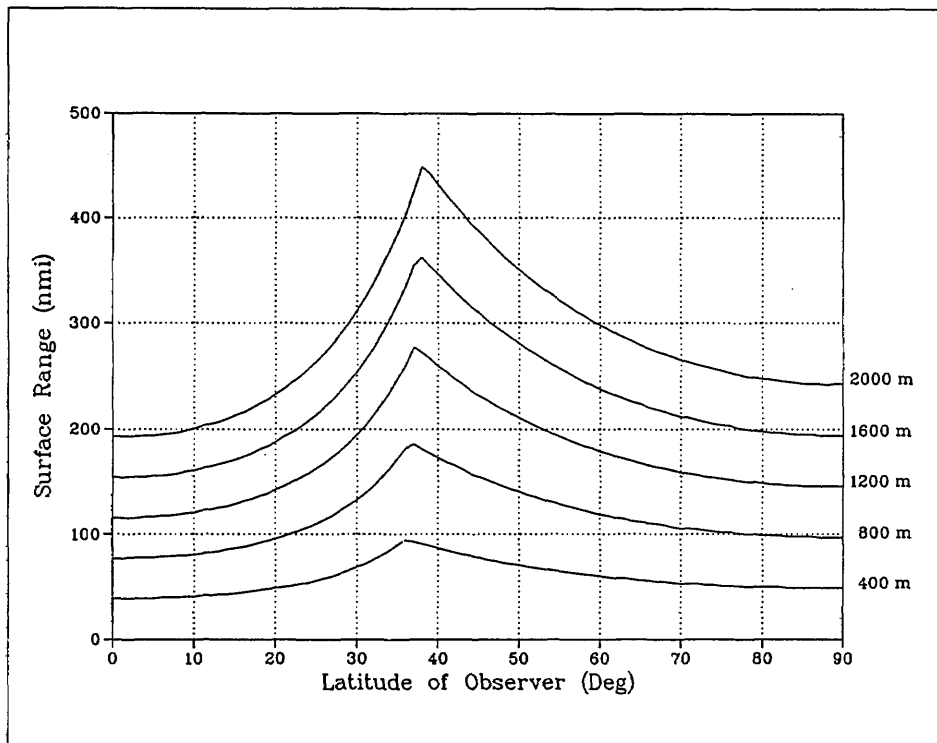


Fig. 10 — Spherical Approximation range error contours vs observer latitude

Having established the superiority of the Midpoint Flat Earth model, we now question in which regions it is safe to use this model before using a spherical model such as the Spherical Approximation model. Figure 9 shows the Spherical Approximation model contours. The 1-nmi error contour shows the distance to which one can go to incur not more than a 1-nmi error at any latitude north of the equator. Thus, for example, if an observer is at 15°N and if the distance between the observer and a second point is less than or equal to 200 nmi, distances can be computed accurately to within 1-nmi. A 2-nmi error is incurred at 15°N at distances up to approximately 380 nmi, and so forth. The contours of Fig. 9 indicate that the Spherical Approximation to the WGS-84 ellipsoid is best in the region from 38°N to about 42°N. Comparison of the contours in Fig. 8 and those in Fig. 9 are now performed to determine the regions where switching from the Midpoint Flat Earth model to Spherical Approximation model should take place. By comparing the 1-nmi error contour on each figure, we can see that the 1-nmi error contour in Fig. 9 begins to allow for greater distance calculations at 36°N and 375 nmi. Essentially, this is the crossover point where the Spherical Approximation model yields an improved representation. Similar comparisons for the other four contours yield the following approximate crossover points:

Surface Error (nmi)	Latitude (°N)	Distance (nmi)
1	36	375
2	65	500
3	39	1050
4	35	1125
5	29	1250

Below 29°N latitude there appears to be a 0.5-nmi difference between the two models in favor of the Midpoint Flat Earth model. Beyond that, the Spherical Approximation can maintain a better approximation to the WGS-84 ellipsoid model:

Figure 8 should not be interpreted to mean that a flat Earth model is adequate over distances of 1000 nmi. In practice, however, most applications should hold the differences to under 1 nmi. This indicates that a distance of 200 nmi is the practical extent over which calculations can be performed with such a representation. Since the Spherical Approximation model yields approximately equivalent errors up to about 80°N (beyond which this model is superior to the Midpoint Flat Earth model), considerations to use the Spherical Approximation at all latitudes for distances of less than 200 nmi are strong. This trade-off, however, is performed based on timing considerations between the two approaches. Finally, Fig. 10 shows a fine-grain analysis (under 1-nmi error). A 1000-m error will not be exceeded by not exceeding distances of 220 nmi (that is, approximately 1 part in 440). This then yields a practical limitation on the regions over which the Midpoint Flat Earth model could safely be used below 80°N. Above 80°N no flat Earth representation is adequate.

#### *Comparison of Spherical Approximation Model and WGS-84 Ellipsoidal Model*

By setting an appropriate error budget, plots as shown in Figs. 9 or 10 can be used to determine how far in range we can use the Spherical Approximation model before we must use the WGS-84 ellipsoidal calculations. For example, if an application program is used in the region between 50°N and 60°N with a maximum error tolerance of 2 nmi, we can safely apply the Spherical Approximation model for calculating distances up to 550 nmi. Beyond this distance, we should switch to the WGS-84 ellipsoidal calculations. For 1-nmi error tolerances between 50°N and 60°N the maximum range distance is about 270 nmi.

In summary, many areas of interest lie in the region between 40°N and 70°N. Over this region the Midpoint Flat Earth model yields acceptable results (errors less than 1000 m) at distances under 100 nmi. From 100 nmi to approximately 250 nmi both the Midpoint Flat Earth and the Spherical Approximation models yield similar results. For the distances beyond 250 nmi it is best to use WGS-84 calculations. For example, at 50°N both models yield an error of 1 nmi at a distance of approximately 270 nmi. At a distance of 1000 nmi the Midpoint Flat Earth model yields an error of approximately 6 nmi (Fig. 8) and the Spherical Approximation model gives a 3-nmi error (Fig. 9) at 50°N latitude. Both results are generally beyond acceptable limits.

**Timing Considerations**

Examination of the code of the Geodetic Inverse solution in Appendix A shows that an iterative loop is used to perform the ellipsoidal calculation. Subsequent data in this report show that this loop is repeated only if the semimajor and semiminor axes are not equal; for a sphere, only one pass is made through the loop. When this routine is used for ellipsoids in production applications, this loop can potentially be time consuming. A driver program was written to test the loop and the associated loop tolerance. The observer at point *O* is placed at 0° longitude and 0° latitude. The driver program contains three loops to vary the tolerance, the longitude of the target at point *A*, and the latitude of the target at point *A*. The longitude of point *A* is changed in 1° steps from -179° to +180°. The latitude of point *A* is varied from 0° to 90° in 1° steps. Since the convergence tolerance is directly related to CPU utilization, the loop tolerance is varied from 10<sup>-1</sup> to 10<sup>-12</sup>. The tolerance of 10<sup>-12</sup> is the value used by DMA for applications that require high levels of accuracy. It is used here as a reference to calculate maximum or worst case range measurement errors at the other tolerances. All range- and bearing-error analyses presented earlier in this report use the 10<sup>-12</sup> tolerance for the WGS-84 reference ellipsoid.

Table 2 gives a summary of the test results for the 32760 positional data points calculated. The Δ distance errors vary approximately an order of magnitude as the tolerance varies an order of magnitude.

Table 2 - Maximum Errors from 10<sup>-12</sup> Tolerance

Tolerance	Δ Distance (nmi)	Δ Bearing (deg)
10 <sup>-11</sup>	0.00000003	0.00000001
10 <sup>-10</sup>	0.00000034	0.00000014
10 <sup>-9</sup>	0.00000302	0.00000124
10 <sup>-8</sup>	0.00003398	0.00001044
10 <sup>-7</sup>	0.00034435	0.00008813
10 <sup>-6</sup>	0.00337846	0.00100208
10 <sup>-5</sup>	0.03439104	0.00628367
10 <sup>-4</sup>	0.29504115	0.15386889
10 <sup>-3</sup>	3.42600647	1.30084743
10 <sup>-2</sup>	34.26006474	11.30886079
10 <sup>-1</sup>	36.07383288	180.00000000

Examination of the Geodetic Inverse code in Appendix A shows that an automatic limit of 100 loops is set on each call to the routine. This limit was added as a precaution against cases that converge too slowly. The number of loops actually observed in the testing gives an approximation of the CPU's utilization

required. Table 3 shows a profile of the number of loops for each tolerance magnitude for nonspherical calculations.

Table 3 can also be used to generate probability curves of convergence loop occurrences. From these probabilities we can obtain the associated cumulative probabilities that the number of loops incurred is less than a fixed number. Figure 11 shows a plot of these cumulative probabilities for four of the tolerances tested. The probability of incurring three loops or less with a tolerance of  $10^{-7}$  is approximately 0.85. That is, 85% of the time an ellipsoidal calculation is performed, it requires three or fewer loops at that tolerance. However, to use the software as DMA requires for its purposes (that is, using a tolerance of  $10^{-12}$ ), 85% of the time requires the use of five loops or fewer. Hence it requires twice the amount of looping to improve the results by a tolerance of  $10^{-5}$ .

Table 3 — Inverse Loop Count vs Tolerance Magnitude for WGS-84 Ellipsoid

Looped	$10^{-01}$	$10^{-02}$	$10^{-03}$	$10^{-04}$	$10^{-05}$	$10^{-06}$	$10^{-07}$	$10^{-08}$	$10^{-09}$	$10^{-10}$	$10^{-11}$	$10^{-12}$
1 Time	32760	32760	32760	10674	593	539	539	539	539	539	539	539
2 Times				22086	23922	8520	2554	666	72	4	0	0
3 Times					8180	23260	27830	16700	8220	3960	1846	762
4 Times					54	396	1666	14292	22436	20958	12312	7516
5 Times					6	34	136	464	1228	6652	16712	21356
6 Times					2	6	22	66	192	482	996	1888
7 Times						2	8	20	42	108	238	474
8 Times					2			6	16	30	66	134
9 Times							2	2	8	12	26	48
10 Times						2			2	6	10	18
11 Times								2		4	6	10
12 Times							2		2		2	6
13 Times											2	2
14 Times								2		2		2
15 Times											2	
16 Times									2			
17 Times												2
18 Times										2		
21 Times											2	
23 Times												2
101 Times	0	0	0	0	1	1	1	1	1	1	1	1

A comparison of the data in Table 2 with the contour data in Fig. 9 indicates that using a convergence tolerance of  $10^{-4}$  for the WGS-84 ellipsoid is equivalent to using the Spherical Approximation for surface ranges under 250 nmi. Table 3 shows that the loop count for a tolerance of  $10^{-4}$  is predominantly less than or equal to 2. Hence for applications requiring a range error budget under 1 nmi, a tolerance of  $10^{-4}$  in the ellipsoidal model serves very well.

Data collection was performed to obtain WGS-84 reference ellipsoid timing vs the number of required loops sampled at a loop convergence tolerance of  $10^{-12}$ . Table 4 summarizes the average CPU time on a VAX 8650 for the Inverse and the Direct Solutions (per call to each) as a function of the number of loops each algorithm takes. Only five sets of data were obtained for the Direct Solution. This is due to the low probability of loop counts exceeding 5 for that routine (that is, higher loop counts could not be found).

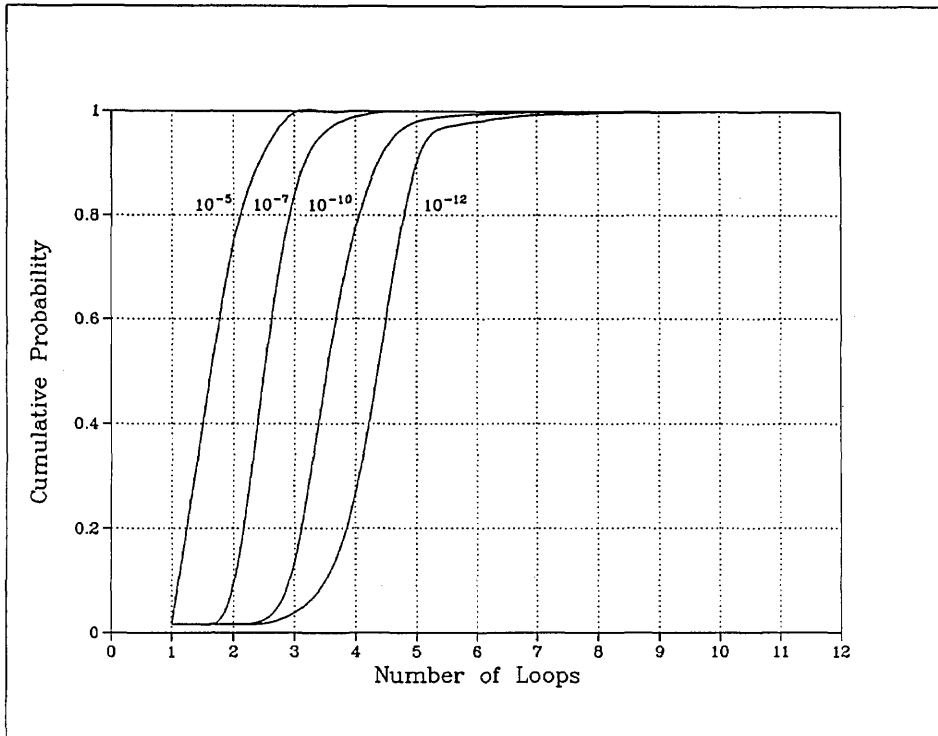


Fig. 11 — Loop count probability

Table 4 — Sample Loop Count Timing for  
WGS-84 Reference Ellipsoid Routines

Loops	Inverse ( $\mu$ s)	Direct ( $\mu$ s)
1	298	261
2	452	353
3	496	406
4	612	432
5	711	530
6	803	—
7	917	—
8	1008	—
9	1133	—
10	1244	—
11	1273	—
12	1368	—
13	1469	—

An associated study of timing to achieve the number of computations discussed in the previous section is now examined. 1° steps in the northern hemisphere are selected to exercise the geodetic subroutines, including one that calculates the chordal distance (Appendix C), 32,760 times. For the other geodetic routines, the observer is placed at seven latitudes, from 0° to 90° in 15° increments, generating 229,320 data points.

VAX 8650 CPU time is extracted for each subroutine call, and Table 5 shows the results. Because the routines are exercised at a uniform distribution (1° steps) in the northern hemisphere, these numbers may be considered good statistical averages.

Table 5 - CPU Time for Each  
Geodetic Calculation

Geodetic Calculation	Per Call ( $\mu$ s)
DMA Chord Subroutine	294.4
End Point Flat Earth Direct	181.0
End Point Flat Earth Inverse	411.6
Midpoint Flat Earth Inverse	200.0
Midpoint Flat Earth Direct	184.0
Spherical Inverse Solution	420.5
Spherical Direct Solution	436.3

The DMA Chord subroutine requires the least amount of time, 294.4  $\mu$ s per call. It is noteworthy that three inverse calculations, two for flat Earth and one for the spherical Earth, take approximately the same amount of time. This shows that replacing a flat Earth model with a spherical Earth model has a minimal impact on CPU time.

Table 6 presents the CPU requirements for the WGS-84 ellipsoid loop convergence tolerances ranging from  $10^{-12}$  through  $10^{-1}$ . The CPU utilization drops dramatically as the convergence tolerance is lessened. Table 3 shows the reduction in convergence looping as a result of this tolerance reduction. Table 4 shows the corresponding reduction in CPU time as a function of the number of loops. Thus we can readily predict the resulting tendencies as shown in Table 6.

Using all of the aforementioned tables and figures, we can now perform an Earth model selection process. As an example, the ENEWS Program generates digital computer representations of large scale EM environments with ship, aircraft, and missile motion. These representations, referred to as scenarios, currently extend over distances of up to 800 nmi. Ships, missiles, and aircraft are considered as mass points; their dimensionality is considered only when radar cross section is calculated. An assumption of an error budget of under 1 nmi (a distance of the order of magnitude of approximately six times the length of a Navy carrier) leads to the requirement of using a convergence loop tolerance of  $10^{-4}$  or less (Table 2) when using the WGS-84 reference ellipsoid calculations. Since, in scenario motion computations, the Direct Geodetic Solution is the one predominantly used, the discussion focuses only on values for this computation. Table 7 is extracted from Tables 2, 5, and 6 and Fig. 9.

Table 6 — CPU Time Per Call for Each Convergence Tolerance for the WGS-84 Reference Ellipsoid

Convergence Tolerance	Inverse ( $\mu\text{s}$ )	Direct ( $\mu\text{s}$ )
$10^{-12}$	747.2	697.9
$10^{-11}$	693.8	633.7
$10^{-10}$	662.0	627.1
$10^{-09}$	651.1	591.6
$10^{-08}$	610.0	574.9
$10^{-07}$	578.7	569.8
$10^{-06}$	551.3	523.2
$10^{-05}$	517.7	510.9
$10^{-04}$	495.8	506.1
$10^{-03}$	464.2	455.5
$10^{-02}$	405.0	424.6
$10^{-01}$	413.0	428.9

Table 7 — Timing and Error Considerations for Spherical Approximation and Selected WGS-84 Loop Tolerances

	CPU Time per call ( $\mu\text{s}$ )	Maximum Distance Error from WGS-84 Ellipsoid ( $10^{-12}$ ) at 800 nmi	
		(m)	(nmi)
Spherical Approximation	436.3	7408	4.0
WGS-84 ( $10^{-4}$ )	506.1	546	0.295
WGS-84 ( $10^{-5}$ )	510.9	63	0.034

The incurred Spherical Approximation model distance error is taken over all latitudes. Restricting the error to latitudes between  $40^\circ\text{N}$  and  $70^\circ\text{N}$  still yields an error of approximately 3 nmi at a surface range of 800 nmi. This range measurement error far exceeds the allotted error budget. Figure 9 shows that it is impossible to achieve the desired error budget under 1 nmi at distances of 800 nmi. Thus, this narrows the model selection choice to the use of the WGS-84 calculations with a 13.5 factor improvement in the resultant error (0.295 nmi vs 4 nmi) at a cost of only 70  $\mu\text{s}$  more per subroutine call. The choice of a tolerance of  $10^{-5}$  rather than  $10^{-4}$  yields an improvement factor of approximately 118 times (0.034-nmi error vs 4 nmi) at a cost of only 4  $\mu\text{s}$  more per call than at the  $10^{-4}$  tolerance. It is clear that the most cost effective choice of Earth model to use for the scenario application described above is the WGS-84 reference ellipsoid model that uses a convergence loop tolerance of  $10^{-5}$ . For scenarios covering smaller distances, either a larger tolerance for the WGS-84 reference ellipsoid or the Spherical Approximation model may be used. Thus, for example, for a 250-nmi coverage (see Fig. 9) a 1-nmi error budget is achieved at a cost reduction of  $506.1 - 436.3 = 69.8 \mu\text{s}$  per call (Table 7).

## Summary

To summarize the Earth model selection process in a general manner, a nomogram of the distance coverage, error budget, and additional CPU timing costs is constructed for the latitudes 0°N through 70°N. The latitudes are separated into two belts, the equatorial region (0°N to 40°N) and the midlatitudes (40°N to 70°N). This is accomplished by constructing Table 8 from the preceding tables and figures. Timing costs shown in units of microseconds are CPU time in addition to the time required to compute the direct Midpoint Flat Earth (MPFE) model calculation. The distances in the table are the maximum distance computed under the constraint of the associated maximum error. For example, the Spherical Approximation (SA) model can be used up to a distance of 250 nmi with a maximal error of 1 nmi in the midlatitude regions at a cost of 252  $\mu$ s above the time required for an MPFE direct calculation. Figure 12 is then constructed from the data in Table 8. The nomogram is constructed for the purpose of serving as an Earth model selection tool. It provides the means for determining possible distance coverages within specified range error budgets with associated CPU utilization costs that are additional to those incurred by using the MPFE model. To gain an understanding of how to use this nomogram, the reader must work through the inferences drawn from it in the next paragraph.

From the nomogram, with the WGS-84 reference ellipsoid represented by all the shaded regions, we can infer the following:

1. The SA model cannot be used to compute a distance of more than 250 nmi with a 1-nmi error budget; nor can the MPFE model. Only the WGS-84 operating at a convergence tolerance of  $10^{-3}$  or less can be used.
2. The MPFE model actually outperforms the SA model (as previously discussed) in the equatorial region. However, it is limited to a distance coverage of 720 nmi for error budgets under 3.42 nmi. For an additional cost of 271  $\mu$ s, this limitation is alleviated by the use of the WGS-84 model at  $10^{-3}$  convergence loop tolerance. Within an error budget of 0.295 nmi, a switch must be made to a tolerance of  $10^{-4}$  at a cost of an additional 51  $\mu$ s per subroutine call.
3. For distances greater than 500 nmi and error budget greater than 3.42 nmi, the SA model is superior to the MPFE model at midlatitudes. However, the WGS-84 reference ellipsoid model outperforms the SA model by 11  $\mu$ s per call with no distance limitation. Thus, for these error budgets, the SA model is not cost effective in comparison to the WGS-84 model.
4. For budget tolerances under 0.295 nmi there is very little difference in coverage between the SA model and the MPFE model, with an attendant maximum coverage of 75 nmi. The WGS-84 reference ellipsoid model operating at  $10^{-4}$  convergence loop tolerance provides an unlimited coverage at an additional CPU time cost of 322  $\mu$ s.

## APPLICATION TO ENEWS SIMULATIONS

By necessity, ENEWS must be responsive in performing EW assessments because of more complex and changing technologies. Such technologies include the use of satellites, enhanced interferometry, as well as improvements in EW systems due to the extensive integration of on board computers and microprocessors as part of these systems. The Earth models must be chosen so that they serve as adequate vehicles with which to conduct studies, the results of which fall within acceptable error-tolerance levels. Clearly, the inclusion of dynamic Earth satellites precludes the use of any flat Earth models.

Table 8 — Distance Coverages and Additional CPU Timing Costs

Maximum Error Budget (nmi)	Distance Coverage (nmi)	WGS-84				SA		Timing Cost ( $\mu$ s)	MPFE		Timing Cost ( $\mu$ s)
		Timing Cost ( $\mu$ s)				Distance Coverage (nmi)			Distance Coverage (nmi)		
		$10^{-5}$	$10^{-4}$	$10^{-3}$	$10^{-2}$	0°N - 40°N	40°N - 70°N	0°N - 40°N	40°N - 70°N		
- 0.034		327									
0.034 - 0.295	Coverage	322				50	75	252	52	60	0
0.295 - 1.0	Over					187	250		203	245	
1.0 - 2.0	Any					360	490		420	450	
2.0 - 3.0	Distance					547	730		620	500	
3.0 - 3.42	in the					600	820		720	510	
3.42 - 4.0	Northern					705	970	812	525		
4.0 - 5.0	Hemisphere					910	1200	1030	575		
5.0 -											

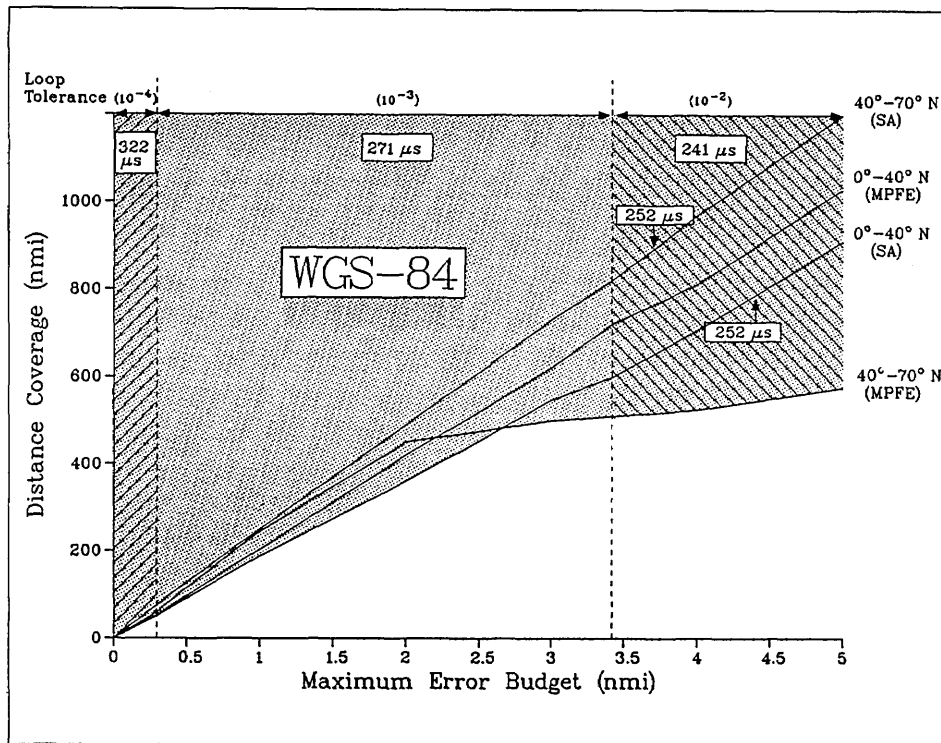


Fig. 12 — Distance coverage and additional CPU timing costs

The selection process of an Earth model for current and future applications within the ENEWS Program rests between the use of a spherical Earth model, such as the Spherical Approximation model, or an ellipsoid of revolution, such as the DoD standard World Geodetic System. Since the CPU timing between the two methods is effectively equivalent, timing does not contribute to the decision process. The remaining factors are accuracy and computer programming considerations.

First we address the question of accuracy and data sources. As this report shows, accuracies of at best 3.5 to 4 nmi can be achieved for distances at and beyond 800 nmi by using the Spherical Approximation model. At the same distance, the WGS approach yields accuracies that are less than 0.3 nmi from the DoD standard. This is a significant difference for applications that require the placement of surface to air missile (SAM) sites and any other target elements. Generally, ENEWS receives site data from sources such as the

Electronic Order of Battle (EOB) and the Air Order of Battle (AOB). These data are obtained primarily from maps that use local datums (that is, local national surveys). If local surveys are not available, point positions are drawn from the WGS system. Thus, these local datums are generally not consistent with each other. For problems covering transoceanic or even intercontinental distances, this problem is very apparent. The WGS standard provides the transformation to convert specific local coordinates into the WGS system and vice versa [2]. However, the differences in point location between using local datums and WGS-84 varies generally from 200 m to 1 or 2 nmi. Consequently, WGS-84 provides a consistent model that covers large distances with site coordinate data and with known maximal variations from the actual location. A spherical Earth model does not ensure this consistency over more than a single datum.

For the problems that involve ground based radars, local terrain elevation features play an essential role in determining masking effects, that, in turn, affect the contributions to observable pulse densities in EM environments. DMA provides Digital Terrain Elevation Data (DTED) for most land masses. These data are referenced to the WGS-84 system. ENEWS has developed software to retrieve and process DTED [4] and currently maintains a database covering regions of interest. Also, many vendor-supplied mission-planning-graphics software tools use DTED for determining elevations and line of sight. Attempting to use DTED for such analyses with spherical Earth models causes a misplacement of geographic features by several miles. This would result in distortions of resultant pulse densities attributable to many ground sites as viewed from long distances.

Finally, from the programming consideration viewpoint, it is important to achieve maximum flexibility to be able to solve future problems while incurring minimum impact in programming implementation. It is a fact that the Direct and Inverse Solution software implementation is identical for the Spherical Approximation model as well as for the WGS-84 model. Since the Spherical Approximation model, or for that matter any spherical Earth model, is valid only in a local sense (that is, over limited number of contiguous datums), these do not offer the desired flexibility needed in future growth in solving EW problems.

## CONCLUSIONS

The following conclusions may be drawn from the previous analyses:

1. End Point Flat Earth models are inadequate representations of the Earth even over short ranges (less than 100 nmi.) However, other flat Earth models such as the Midpoint Flat Earth model may be adequate for many applications.
2. Flat Earth models should not be used to calculate distances greater than 100 nmi, especially north of 40°N latitude if attempting to achieve less than 1000-m accuracies.
3. The Spherical Approximation model, on the average, yields an equivalent if not better representation than the Midpoint Flat Earth model over most of the globe. This type of model can serve adequately for distances up to approximately 250 nmi in the 40°N to 70°N regions while incurring differences less than 1000 m with respect to the WGS-84 ellipsoid.
4. Beyond previously indicated ranges, the WGS-84 model should be used. Data indicate that four convergence loops or fewer would be incurred approximately 95% of the time that Geodetic Inverse Solutions are performed. On the average, one call for a Geodetic Inverse Solution requires 0.5 ms on a VAX 8650. The Direct Solution requires, on the average, 0.363 ms.

For the accuracies achieved, and, in view of the constant improvement in the CPU throughput of new machines, the CPU utilization is a minimal and decreasing parameter in the Earth model selection process. Tolerances can be "tightened" if necessary with the arrival of faster digital computers.

5. For accuracy requirements under 1 nmi, the WGS-84 reference ellipsoid used with a convergence loop tolerance of  $10^{-5}$  over all ranges on a hemisphere is the most cost effective Earth model selection for ENEWS scenario applications.

## RECOMMENDATIONS

As a result of the preceding analyses and conclusions, it is evident that the choice of an Earth model based on allowable range errors is the prime factor in this decision-making process. Loss of accuracy in geodetic computations negates the validity of any study being performed. If such studies are consistently performed over ranges not exceeding 100 nmi, then any of the Earth models presented here is adequate. However, satellite applications with appropriate motion cannot be included in any flat Earth model approach. Hence, flat Earth models must be excluded from further considerations in solving problems that will arise in the 1990s.

The WGS system is an Earth model that offers point positioning control on a global basis. Although large differences may exist even between contiguous datums, such differences can be handled uniformly. Spherical Earth models offer no resolution to this problem. Consequently, for all the reasons cited, it is recommended that the ENEWS Program embark on enhancing its scenario environment generator by using the DoD-wide standard WGS model to perform all required geodetic calculations.

## ACKNOWLEDGMENTS

The authors thank Dr. Muneendra Kumar and Mrs. Caroline Leroy (DMA) for providing the necessary documentation, software, and consultative support to ENEWS, NRL. The authors also thank Mr. Willard Dahl (ENEWS), Dr. Allen Duckworth (ENEWS), and Mr. Donald Grady (ENEWS Program Manager) for their helpful suggestions in the preparation of this report. Special acknowledgment is given to Dr. Ronald Brown (ENEWS) for verifying the WGS-84 formulae implementation.

## REFERENCES

1. Jordan-Eggert, *Jordan's Handbook of Geodesy* (Army Map Service, 1962), Volume III, First Half (English translation by Martha W. Carta, Section 44).
2. Defense Mapping Agency Technical Report, DMA TR 8350.2, "Department of Defense World Geodetic System 1984—Its Definition and Relationships with Local Geodetic Systems," Sept. 1987, pp. 7-9.
3. Defense Mapping Agency Technical Report, DMA TR 80-003, "Geodesy for the Layman," Dec. 1983, p. 8.
4. Leroy, S.S. "Introduction to the ENEWS DTED Software Retrieval System," ENEWS Report, Apr. 1989.

## Appendix A

### THE GEODETIC INVERSE SOLUTION SUBROUTINE

This appendix shows the Geodetic Inverse Solution subroutine used for the calculations done in this report. The original code for this routine was obtained from the Defense Mapping Agency (DMA), for which the authors are indebted.

Essentially, this routine has as input the latitudes and longitudes of the two points *O* and *A* on the ellipsoid defined in Fig. 1 in the body of this report. It calculates the surface or arc length in meters, and the *O* to *A* and *A* to *O* bearings in seconds. Fixed constants are defined or generated externally to the routine and passed into the routine in the "Ellipsoid" common block. These formulae are accomplished with double precision accuracy on the computer. The ellipsoid definition for WGS-84 used with this Inverse Solution is as follows:

$$\begin{aligned}A &= 6378137 \\F &= 1. / 298.257223563 \\B &= (1 - F) * A\end{aligned}$$

The following constants are used in the inverse and related geodetic routines not shown here, and are calculated once during initialization for optimum efficiency.

$$\begin{aligned}ASQR &= A * A \\BSQR &= B * B \\BSQOASQ &= BSQR / ASQR \\BOA &= B / A \\FF1 &= 1 - BOA \\F2 &= (ASQR / BSQR) - 1 \\FF16 &= FF1 / 16 \\RTS &= 206264.806247\end{aligned}$$

The code used for the Inverse Solution is shown in the following text. The "&" symbol represents a line continuation. Inputs and outputs are currently given in seconds for angles and in meters for distances.

PICH AND LEROY

SUBROUTINE INVERSE(OLATS,OLONS,OAAZ,ALATS,ALONS,AOAZ,ARC)

C SUBROUTINE INVERSE CALCULATES THE ARC LENGTH BETWEEN POINTS A  
 C AND THE OBSERVER AT POINT O, THE BEARING FROM POINT A TO  
 C POINT O, AND THE BEARING FROM THE OBSERVER TO POINT A.

C GEODETIC INVERSE COMPUTATION BY T. VINCENTY JAN 84

C INPUTS:

C A - SEMIMINOR AXIS IN METERS  
 C B - SEMIMINOR AXIS IN METERS  
 C OLATS - LATITUDE OF POINT O IN SECONDS  
 C OLONS - LONGITUDE OF POINT O IN SECONDS  
 C ALATS - LATITUDE OF POINT A IN SECONDS  
 C ALONS - LONGITUDE OF POINT A IN SECONDS

C OUTPUTS:

C ARC - SURFACE ARC LENGTH BETWEEN POINTS A-O IN METERS  
 C OAAZ - BEARING OF POINT A FROM POINT O IN SECONDS  
 C AOAZ - BEARING OF POINT O FROM POINT A IN SECONDS

IMPLICIT REAL\*8(A-H,O-Z)  
 REAL\*8 LAM, L, K

EQUIVALENCE (K,LAM)

COMMON /ELLIPSOID/ A, B, ASQR, BSQR, BSQOASQ, F, F2, FF1,  
 & FF16, BOA, RTS, DPI, TOLINV, TOLDIR,  
 & SPHERENAME, MAXSPHERES, NRSPPHERE, NRSP,  
 & KLOOP

REAL\*8 A, B, ASQR, BSQR, BSQOASQ, F, F2, FF1, FF16  
 REAL\*8 RTS, DPI, TOLLOOP  
 INTEGER\*4 MAXSPHERES, NRSPPHERE, NRSP, KLOOP  
 CHARACTER\*22 SPHERENAME

C A - SEMIMINOR EARTH AXIS (METERS)  
 C B - SEMIMINOR EARTH AXIS (METERS)  
 C ASQR - A SQUARED  
 C BSQR - B SQUARED  
 C BSQOASQ - CONSTANT = B SQUARED OVER A SQUARED  
 C FF1 - CONSTANT = 1 - F  
 C FF16 - CONSTANT = FF1 / 16  
 C F2 - CONSTANT = (A SQUARED / B SQUARED) - 1  
 C BOA - CONSTANT = B OVER A = B / A  
 C RTS - RADIANS TO SECONDS CONVERSION FACTOR  
 C TOLINV - INVERSE PROGRAM LOOP LIMIT TOLERANCE  
 C TOLDIR - DIRECT PROGRAM LOOP LIMIT TOLERANCE  
 C DPI - DOUBLE PRECISION PI  
 C SPHERENAME - THE NAME OF THE CURRENT SPHERE SELECTED  
 C MAXSPHERES - THE MAXIMUM NUMBER OF SPHERES ALLOWED  
 C NRSPPHERE - NUMBER OF THE CURRENT SPHERE SELECTED  
 C NRSP - THE CURRENT NUMBER OF SPHERES DEFINED  
 C KLOOP - INVERSE LOOP COUNTER

```
DATA TOLINV / 1.D-12 /
```

```
IF ( ALATS .EQ. OLATS .AND. ALONS .EQ. OLONS ) THEN
  ARC = 0.D0
  AOAZ = 0.D0
  OAAZ = 0.D0
  RETURN
ENDIF
```

```
UA = BOA * DSIN(OLATS/RTS) / DCOS(OLATS/RTS)
UB = BOA * DSIN(ALATS/RTS) / DCOS(ALATS/RTS)
COSUA = 1.D0 / DSQRT( UA**2.D0 + 1.D0 )
SINUA = UA * COSUA
COSUB = 1.D0 / DSQRT( UB**2.D0 + 1.D0 )
L = (OLONS - ALONS) / RTS
LAM = L
S = COSUA * COSUB
BAZ = S * UB
FAZ = BAZ * UA
KLOOP = 0
```

```
280 CONTINUE
```

```
KLOOP = KLOOP + 1
IF ( KLOOP .GT. 100 ) THEN
  WRITE(14,*) ' LOOP LIMIT COSA =', COSA
  WRITE(14,*) ' OLATD =', OLATS / 3600.
  WRITE(14,*) ' OLOND =', OLONS / 3600.
  WRITE(14,*) ' ALATD =', ALATS / 3600.
  WRITE(14,*) ' ALOND =', ALONS / 3600.
  GOTO 400
ENDIF
```

```
SINLA = DSIN(LAM)
COSLA = DCOS(LAM)
UA = COSUB * SINLA
UB = -SINUA * COSUB * COSLA + BAZ
SINT = DSQRT( UA**2.D0 + UB**2.D0 )
COST = S * COSLA + FAZ
TH = DATAN2(SINT,COST)
SINA = S * SINLA / SINT
COSA = -SINA**2.D0 + 1.D0
IF ( COSA .EQ. 0.D0 ) THEN
  COSTM = COST
ELSE
  COSTM = -2.D0 * FAZ/COSA + COST
ENDIF
```

```

  C = ( (-3.D0*COSA + 4.D0) * FF1 + 4.D0) * COSA * FF16
TEST = LAM
LAM = (((COSTM**2.D0 * 2.D0-1.D0) * COST * C + COSTM) *
&      SINT*C+TH) * SINA * FF1 * (1.D0 - C) + L
IF ( DABS(TEST-LAM) .GT. TOLINV ) GOTO 280
```

PICH AND LEROY

400 CONTINUE

C \*\*\*\* CALCULATE THE BEARING FROM POINT A TO THE OBSERVER

```

BAZ = DATAN2(-COSUA * SINLA, COSUB * SINUA - BAZ * COSLA )
AOAZ = BAZ * RTS
IF ( AOAZ .LT. 0.D0 ) AOAZ = AOAZ + 1.296D+06

```

C \*\*\*\* CALCULATE THE BEARING FROM THE OBSERVER TO POINT A

```

FAZ = DATAN2(UA,UB)
OAAZ = FAZ * RTS
IF ( OAAZ .LT. 0.D0 ) OAAZ = OAAZ + 1.296D+06

```

```

K = F2 * COSA
C = (((K*(-175.D0)+320.D0)*K-768.D0)*K+4096.D0)
& * K/16384.D0+1.D0
D = (((K*( -47.D0)+ 74.D0)*K-128.D0)*K+ 256.D0)* K/ 1024.D0
S = ( ( ( COSTM**2.D0 * 4.D0 - 3.D0 )
& * ( SINT**2.D0 * 4.D0 - 3.D0 )
& * COSTM * (-D) / 6.D0
& + ( COSTM**2.D0 * 2.D0 - 1.D0 )
& * COST ) * D / 4.D0 + COSTM )
& * SINT * (-D) + TH
ARC = S * C * B
RETURN

```

END

## **Appendix B**

### **THE GEODETIC DIRECT SOLUTION SUBROUTINE**

The Geodetic Direct Solution subroutine is shown in program form on the next two pages. The “&” symbol represents line continuations. Inputs and outputs are given in seconds for angles and in meters for distances. The Direct Solution subroutine calculates the latitude and longitude of an end point, given a beginning point, and the bearing and distance to the end point. The many constants are defined during model initialization as discussed in Appendix A. These constants are passed to the routine by means of the ELLIPSOID.CDK common block that is shown in the listing.

The Direct Solution subroutine also contains an iterative loop like the Inverse routine. The Direct Solution routine loop begins at statement label 10.

PICH AND LEROY

SUBROUTINE DIRECT(ALAT,ALON,BLAT,BLON,FAZ,BAZ,S)

C GEODETIC POSITION COMPUTATION

C INPUTS:

C A - SEMIMINOR EARTH AXIS (IN COMMON)  
 C B - SEMIMINOR EARTH AXIS (IN COMMON)  
 C ALAT - POINT A LATITUDE  
 C ALON - POINT A LONGITUDE  
 C FAZ - FORWARD BEARING (POINT A TO B)  
 C S - SURFACE DISTANCE

C OUTPUTS

C BLAT - LATITUDE OF POINT B  
 C BLON - LONGITUDE OF POINT B  
 C BAZ - BACK BEARING ( POINT B TO POINT A)

IMPLICIT REAL\*8(A-H,O-Z)  
 REAL\*8 LAM, NUM

C ELLIPSOID COMMON BLOCK

COMMON /ELLIPSOID/ A, B, ASQR, BSQR, BSQOASQ, F, F2, FF1,  
 & FF16, BOA, RTS, DPI, TOLINV, TOLDIR,  
 & SPHERENAME, MAXSPHERES, NRSPPHERE, NRSP,  
 & KLOOP

EQUIVALENCE (SINU,TANU), (AA,D), (BB,LAM), (FIRST,NUM)

DATA TOLDIR / 1.D-12 /

COSAZ = DCOS( FAZ / RTS )  
 SINAZ = DSIN( FAZ / RTS )  
 TANU = ( DSIN(ALAT/RTS) / DCOS( ALAT/RTS) ) \* BOA  
 THA = DATAN2(TANU,COSAZ)  
 COSU = 1.D0 / DSQRT(1.D0 + TANU\*\*2.D0 )  
 SINU = TANU \* COSU  
 SINAL = COSU \* SINAZ  
 COSSAL= 1.D0 - SINAL\*\*2.D0  
 XK = F2 \* COSSAL  
 AA = (((XK\*(-175.D0) + 320.D0) \* XK-768.D0) \* XK+4096.D0)  
 & \* XK / 16384.D0 + 1.D0  
 BB = (((XK\*( -47.D0) + 74.D0) \* XK-128.D0) \* XK+ 256.D0)  
 & \* XK / 1024.D0  
 FIRST = S / B / AA  
 TH = FIRST

```

10  COSTHM= DCOS(2.D0 * THA + TH)
    SINTH = DSIN(TH)
    COSTH = DCOS(TH)
    TEST  = TH
    TH    = (((COSTHM**2.D0 * 4.D0-3.D0)
&          * ( SINTH**2.D0 * 4.D0-3.D0)
&          * COSTHM * (-BB) / 6.D0
&          + (COSTHM**2.D0 * 2.D0 - 1.D0) * COSTH )
&          * BB / 4.D0 + COSTHM) * SINTH * BB + FIRST
    IF ( DABS(TH-TEST) .GT. TOLDIR ) GOTO 10

    TEST = SINU * SINTH - COSU * COSTH * COSAZ
    NUM  = SINU * COSTH + COSU * SINTH * COSAZ
    DEN  = BOA * DSQRT(SINAL**2.D0 + TEST**2.D0)
    BLAT = DATAN2(NUM,DEN) * RTS
    LAM  = DATAN2(SINTH*SINAZ, COSU*COSTH-SINU*SINTH*COSAZ)
    D    = ((-3.D0*COSSAL+4.D0)*FF1+4.D0) * COSSAL * FF16
    BLON = (((COSTHM**2.D0 * 2.D0-1.D0) * COSTH * D + COSTHM)
&          * D * SINTH + TH)
&          * SINAL * FF1 * ( D - 1.D0 ) + LAM
    BLON = ALON - BLON * RTS
    IF ( BLON .GT. .648D06 ) BLON = BLON - .1296D07
    IF ( BLON .LT.-.648D06 ) BLON = BLON + .1296D07
    BAZ  = DATAN2(SINAL,TEST) * RTS
    IF ( BAZ .LT. 0.D0 ) BAZ = BAZ + .1296D07
    RETURN

END

```



**Appendix C**  
**CHORDAL DISTANCE CALCULATION SUBROUTINE**

The Chordal Distance subroutine computes the chordal distance between two given points on the Earth. The inputs are the latitudes and longitudes of these two points as well as their associated elevations. As with the other geodetic routines, certain fixed constants are calculated during program initialization and passed to the routine by means of the ELLIPSOID.CDK common block.

PICH AND LEROY

SUBROUTINE CHORD(OLATR,OLONR,OELEV,ALATR,ALONR,AELEV,DCHORD)

C SUBROUTINE CHORD CALCULATES THE CHORDAL DISTANCE BETWEEN  
C POINT O (THE OBSERVER) AND POINT A IN DOUBLE PRECISION METERS.

C INPUTS:

C OLATR - LATITUDE OF POINT O IN RADIANS  
C OLONR - LONGITUDE OF POINT O IN RADIANS  
C OELEV - ELEVATION OF POINT O IN METERS  
C ALATR - LATITUDE OF POINT A IN RADIANS  
C ALONR - LONGITUDE OF POINT A IN RADIANS  
C AELEV - ELEVATION OF POINT A IN METERS

C OUTPUTS:

C DCHORD- CHORDAL DISTANCE IN METERS

IMPLICIT REAL\*8(A-H,O-Z)

C ELLIPSOID COMMON BLOCK

COMMON /ELLIPSOID/ A, B, ASQR, BSQR, BSQOASQ, F, F2, FF1,  
& FF16, BOA, RTS, DPI, TOLINV, TOLDIR,  
& SPHERENAME, MAXSPHERES, NRSPPHERE, NRSP, KLOOP

OC=(ASQR)/DSQRT(ASQR\*(DCOS(OLATR))\*\*2.D0+BSQR\*(DSIN(OLATR))\*\*2.D0)

OX=(OC+OELEV)\*DCOS(OLATR)\*DCOS(OLONR) ! OBS X-COORD  
OY=(OC+OELEV)\*DCOS(OLATR)\*DSIN(OLONR) ! OBS Y-COORD  
OZ=((BSQOASQ)\*OC)+OELEV)\*DSIN(OLATR) ! OBS Z-COORD

AC=(ASQR)/DSQRT(ASQR\*(DCOS(ALATR))\*\*2.D0+BSQR\*(DSIN(ALATR))\*\*2.D0)

AX=(AC+AELEV)\*DCOS(ALATR)\*DCOS(ALONR) ! POINT A X-COORD  
AY=(AC+AELEV)\*DCOS(ALATR)\*DSIN(ALONR) ! POINT A Y-COORD  
AZ=((BSQOASQ)\*AC)+AELEV)\*DSIN(ALATR) ! POINT A Z-COORD

DCHORD=DSQRT( (OX-AX)\*\*2.D0 + (OY-AY)\*\*2.D0 + (OZ-AZ)\*\*2.D0 )

END

## **Appendix D**

### **FLAT EARTH MODEL ANALYSIS**

Figures D1 through D3 give the range error plots calculated for a fixed range of 100 nmi. In Fig. D1 the curves for the Midpoint and End Point Flat Earth models coincide when the observer is at the equator. However, in Fig. D2 the End Point Flat Earth model calculation peaks at nearly double the equatorial error when the observer is at 45°N latitude. The Midpoint Flat Earth model range errors are reduced in Fig. D2 as compared to those in Fig. D1. At northern latitudes, as shown in Fig. D3, the errors are exorbitant for the End Point Flat Earth model, but they have not changed much in peak value from the low-latitude plots for the Midpoint Flat Earth model. They are approximately 0.5 nmi. From these plots, it is clear that the End Point Flat Earth model range calculations increase in error with the increasing latitude away from the equator.

We now analyze the corresponding bearing errors at the range of 100 nmi. When the observer is at the equator, as in Fig. D4, the End Point Flat Earth model errors are only slightly greater than the midpoint model errors. Figure D5, with the observer located at 45°N latitude, shows the bearing errors coinciding at peaks of approximately 0.85° at the 90° and 270° measurements. However, the Midpoint Flat Earth model values exceed those for the End Point Flat Earth model measurements at most other angles. When the observer is positioned at 75°N, as shown in Fig. D6, this effect is amplified further. Bearing errors near 90° are excessive.

PICH AND LEROY

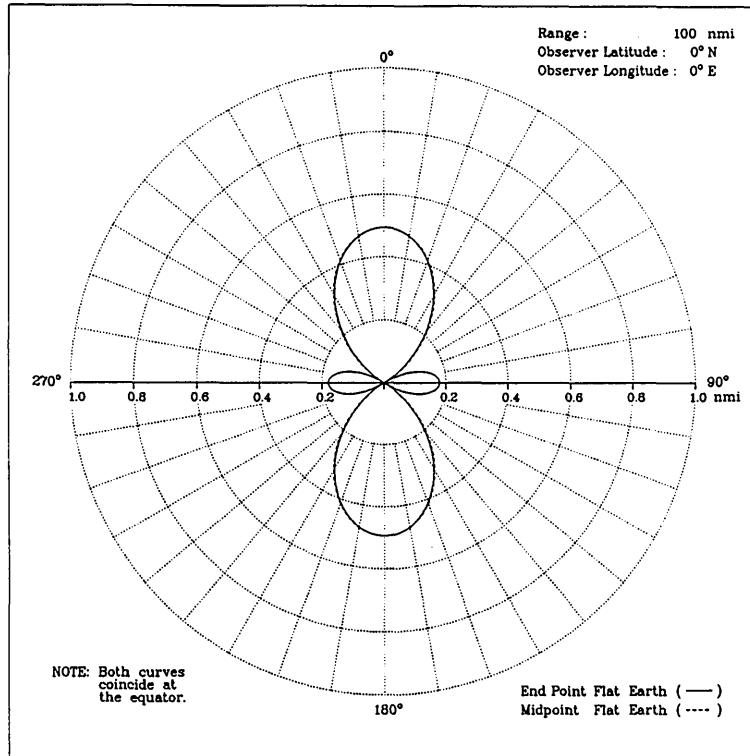


Fig. D1 — Flat Earth range errors vs azimuth

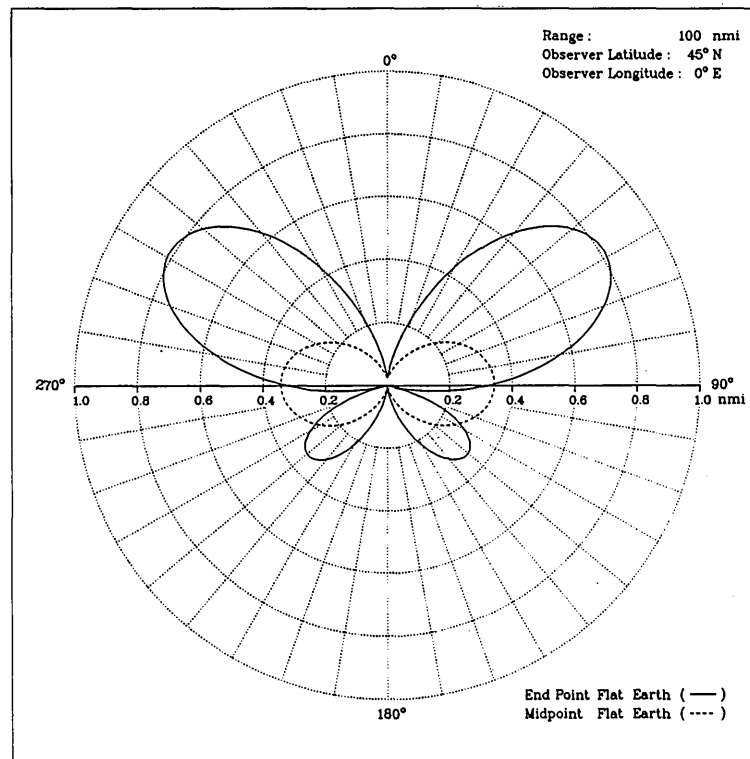


Fig. D2 — Flat Earth range errors vs azimuth

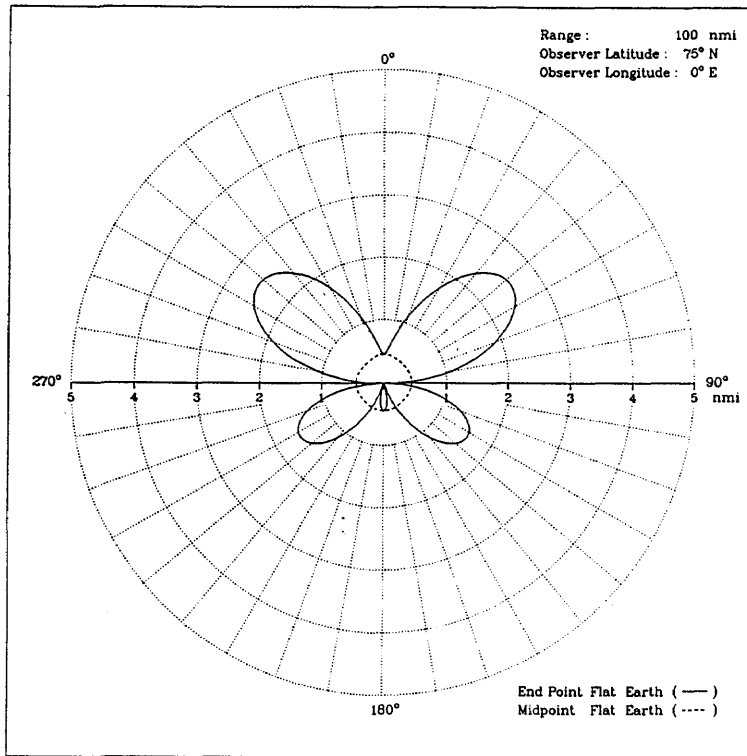


Fig. D3 — Flat Earth range errors vs azimuth

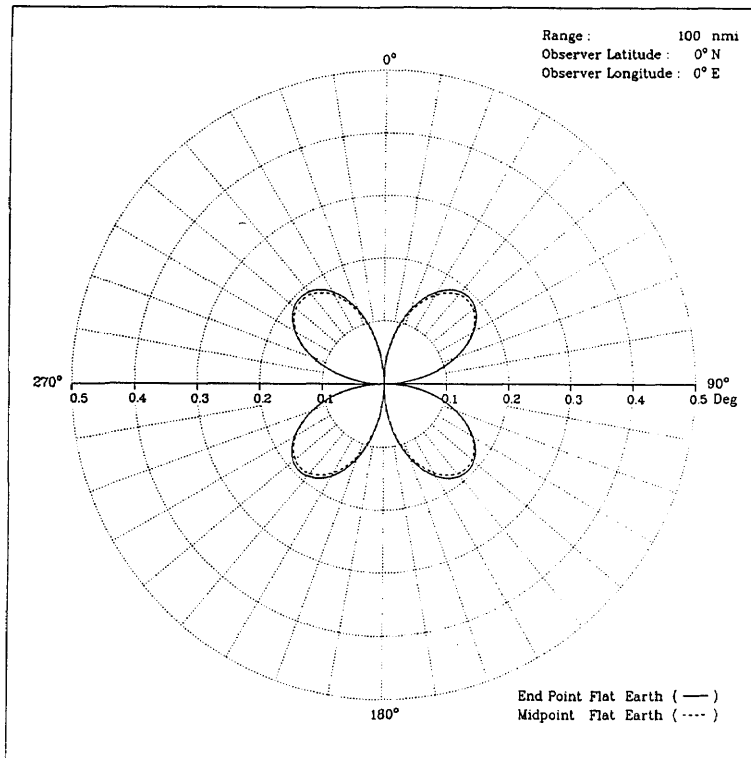


Fig. D4 — Flat Earth bearing errors vs azimuth

PICH AND LEROY

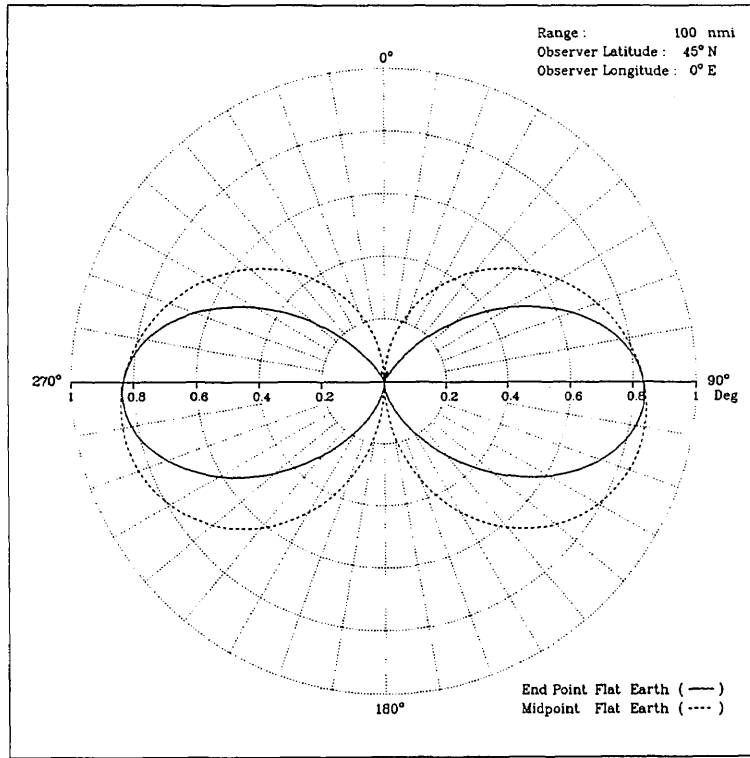


Fig. D5 — Flat Earth bearing errors vs azimuth

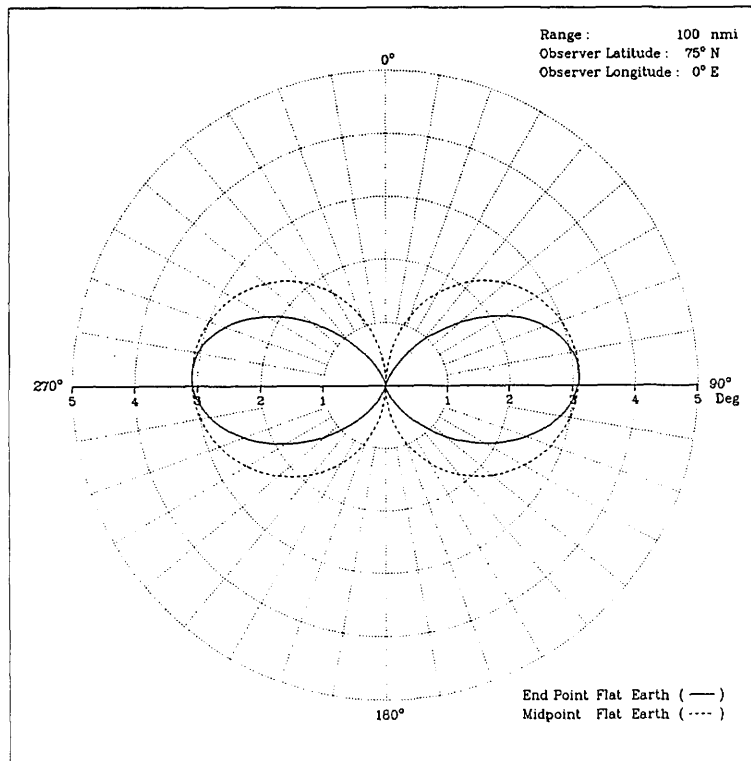


Fig. D6 — Flat Earth bearing errors vs azimuth

## **Appendix E**

### **SPHERICAL EARTH MODEL ANALYSIS**

Figure E1 shows a graph of the selected three spherical models at 500 nmi. The peak error is 2.8 nmi when using the Spherical Approximation. The Navigation Sphere has minimum error at the  $0^\circ$  and  $180^\circ$  azimuths and has maximum error at the  $90^\circ$  and  $270^\circ$  azimuths. The profile of the range errors shown in Fig. E2 changes when the 500-nmi range is used at  $45^\circ\text{N}$ . The Spherical Approximation is predominantly better, except at  $180^\circ$  where the Navigation Sphere is better. In Fig. E3, the range-error curve is nearly circular. The Equal Volume sphere has minimum error over the northern half of the circle, and the Spherical Approximation has least error over the southern half. The Navigation Sphere is consistently worst case. However, all spherical models are within 0.5 nmi in magnitude.

For completeness, errors incurred at longer distances must also be examined. We select a range of 5400 nmi. This represents a distance across a quarter of the Navigation Sphere. Figures E4 through E6 show three latitudes at this range. In Fig. E4, with the observer at the equator, the Spherical Approximation model has the least error, peaking near 6 nmi; the worst error is exhibited by the Navigation Sphere that peaks near 9 nmi. When the observer is moved to  $45^\circ\text{N}$ , Fig. E5 shows error peaks near 20 nmi, and the Navigation Sphere is best to the south of the observer, whereas the Spherical Approximation model is best north of the observer. When the observer is near the pole, at  $75^\circ\text{N}$ , as shown in Fig. E6, the errors are comparatively less, peaking at 9 nmi north of the observer and at 12 nmi south of the observer.

To examine the usefulness of the spherical models at even larger distances, similar calculations were performed at a range of 10,000 nmi. Figure E7 indicates that the Navigation Sphere is worst, and the Spherical Approximation model is best for range error measurement for ranges near 10,000 nmi with the observer at the equator. When the observer is moved to  $45^\circ\text{N}$  latitude, as shown in Fig. E8, errors drop and error profiles change. With the observer at  $75^\circ\text{N}$ , as in Fig. E9, the Spherical Approximation model is consistently the worst of the three models, peaking at 9 nmi and the Navigation Sphere is optimum, peaking at an error of only 3 nmi.

Figures E10 through E12 show bearing errors for observer latitudes of  $0^\circ\text{N}$ ,  $45^\circ\text{N}$ , and  $75^\circ\text{N}$  at a range of 5400 nmi. Bearing errors for the purposes of comparing spherical models are not useful, since these errors from all spheres tested coincide, as can be expected. However, absolute bearing values are of interest. The peak bearing error ( $0.17^\circ$ ) is found in Fig. E11, at  $45^\circ\text{N}$ , whereas maximum errors near the equator and pole are slightly under  $0.1^\circ$ . In all these cases, bearing errors for most modeling applications are insignificant. This observation is also true for a 10,000 nmi range, as shown in Fig. E13. The maximum bearing error is  $0.18^\circ$ .

PICH AND LEROY

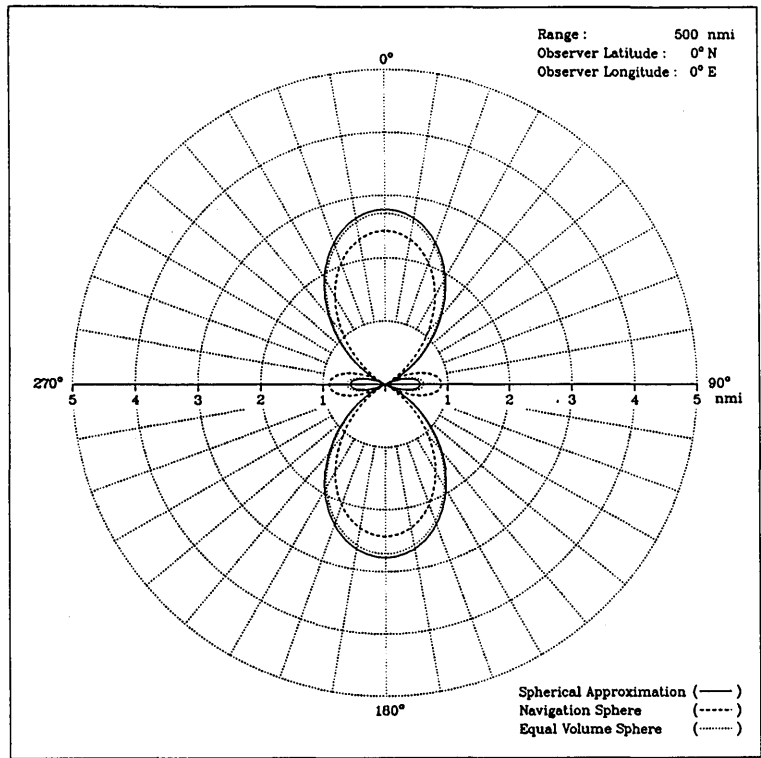


Fig. E1 — Spherical Earth range errors vs azimuth

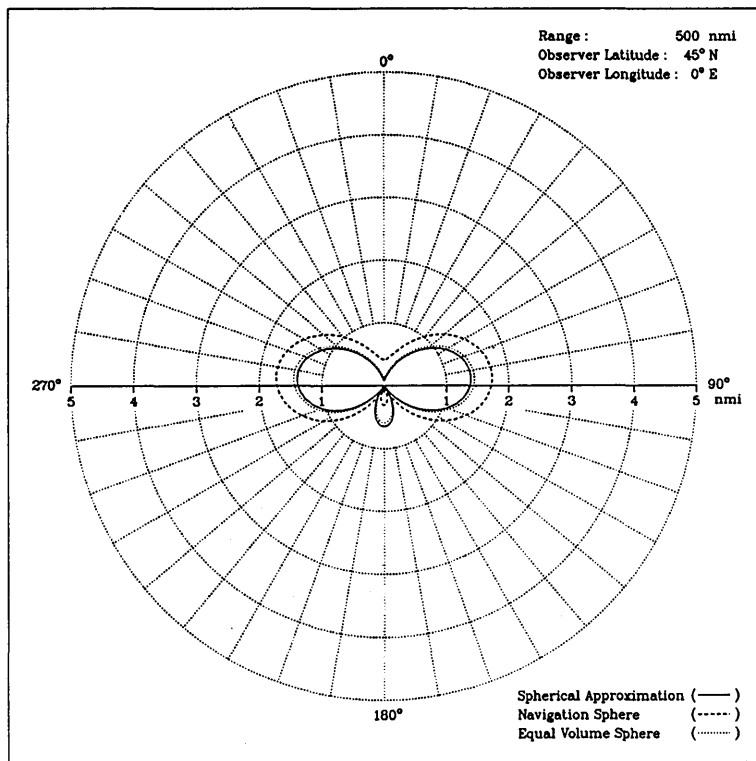


Fig. E2 — Spherical Earth range errors vs azimuth

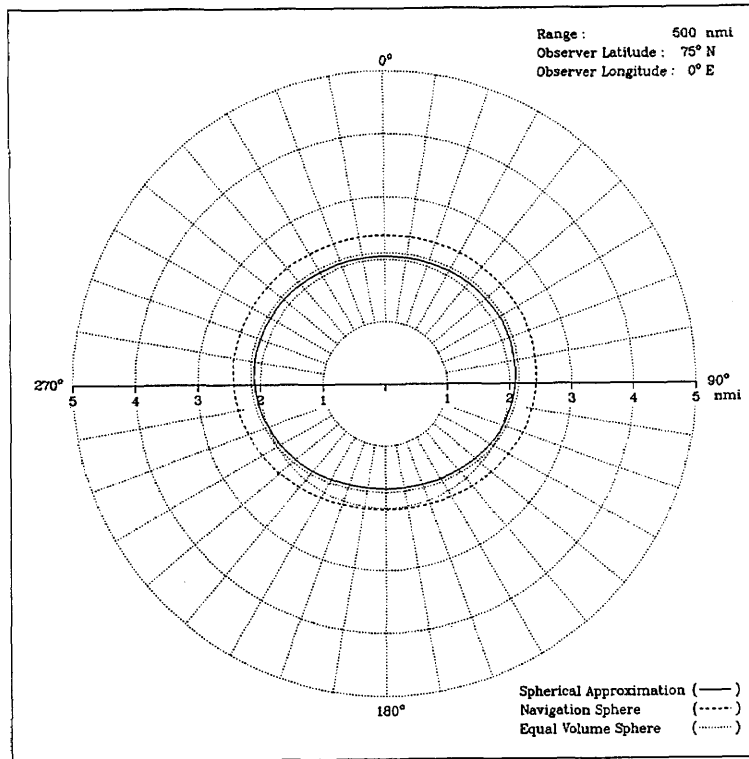


Fig. E3 — Spherical Earth range errors vs azimuth

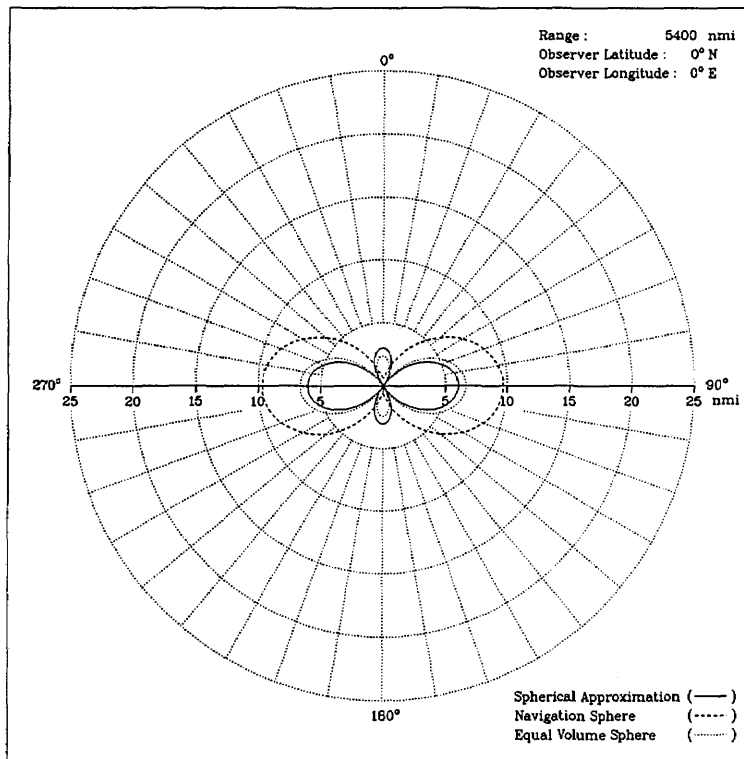


Fig. E4 — Spherical Earth range errors vs azimuth

PICH AND LEROY

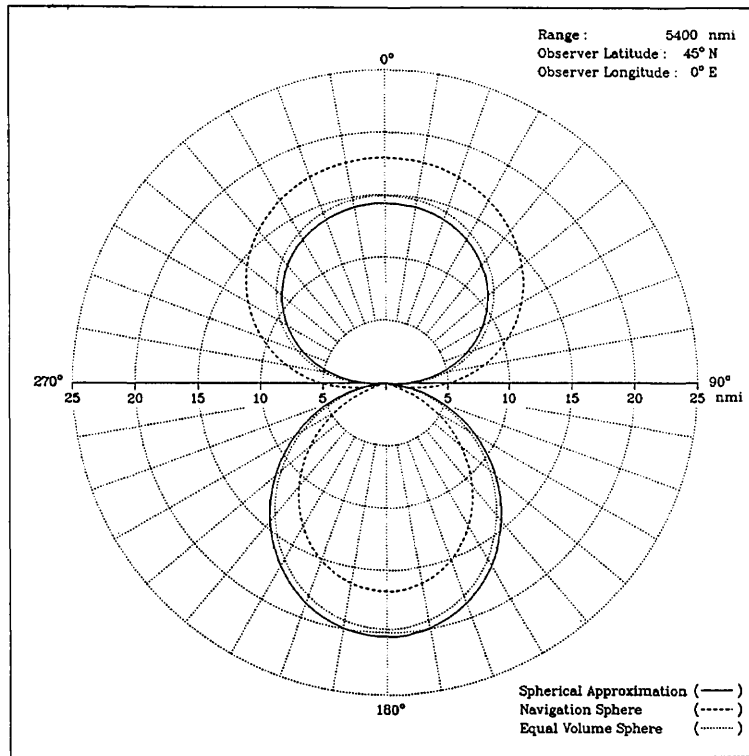


Fig. E5 — Spherical Earth range errors vs azimuth

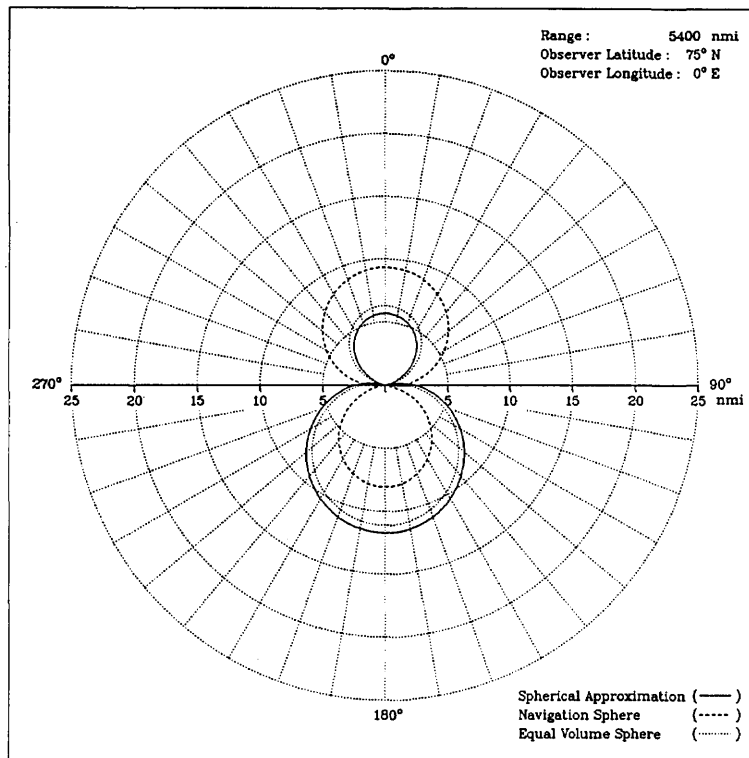


Fig. E6 — Spherical Earth range errors vs azimuth

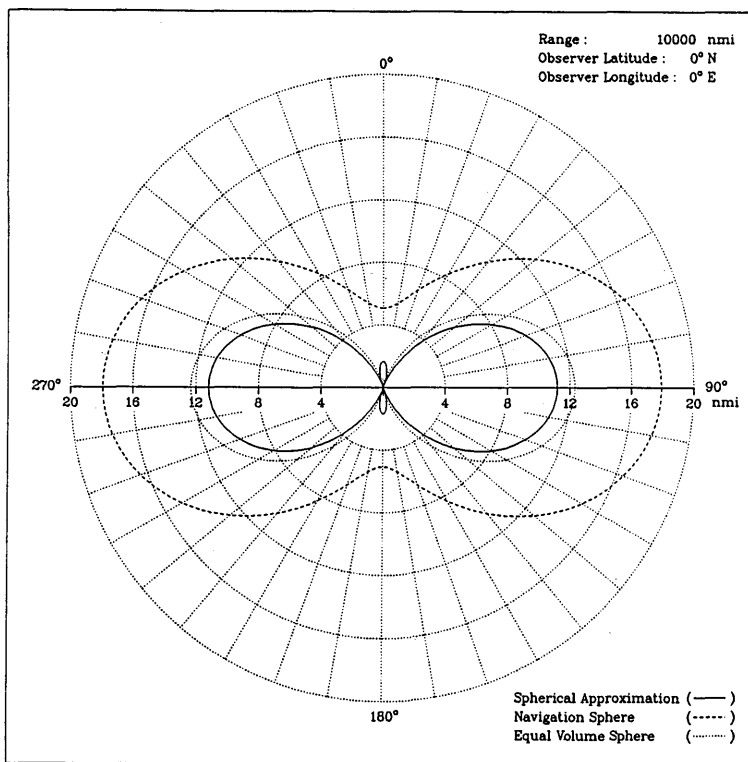


Fig. E7 — Spherical Earth range errors vs azimuth

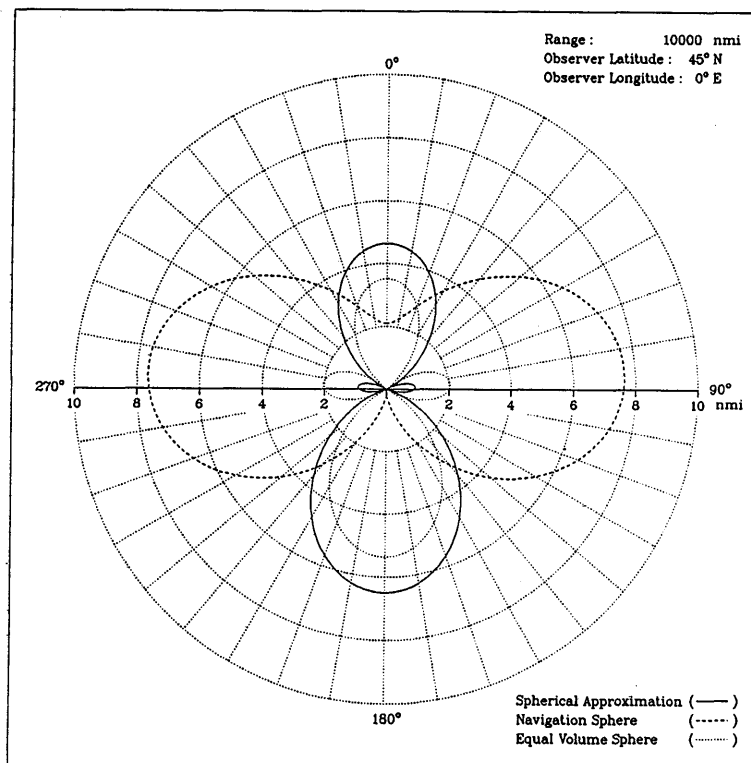


Fig. E8 — Spherical Earth range errors vs azimuth

PICH AND LEROY

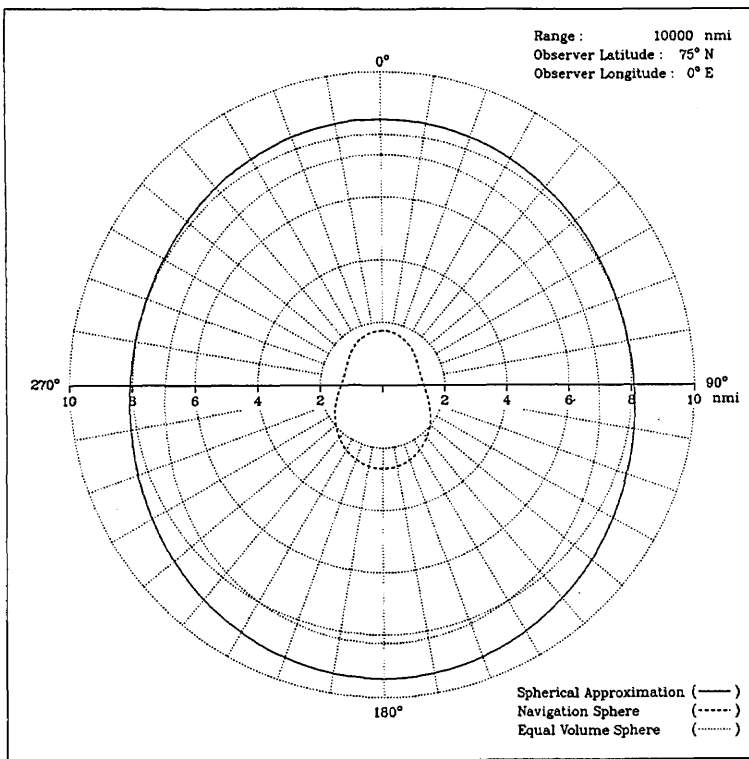


Fig. E9 — Spherical Earth range errors vs azimuth

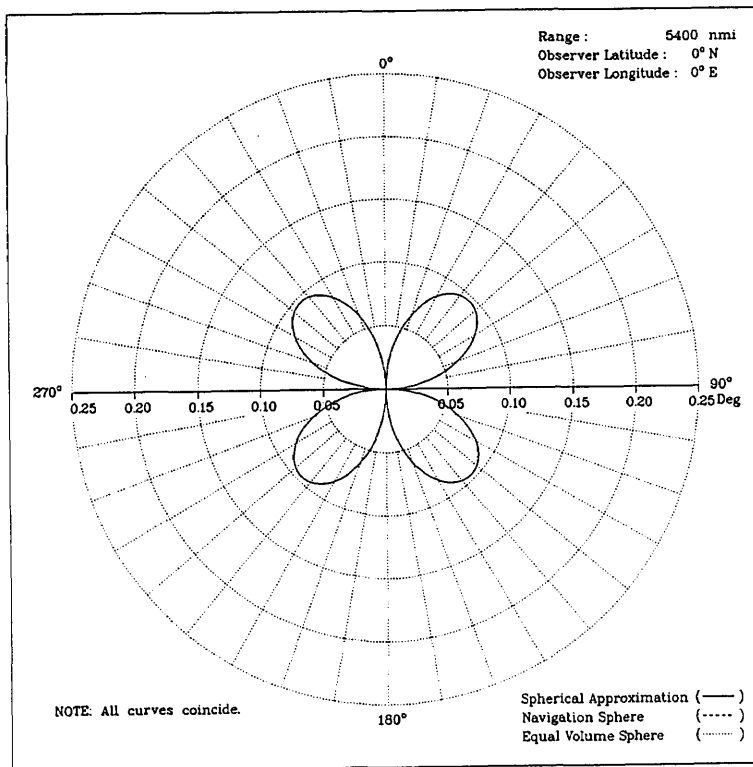


Fig. E10 — Spherical Earth bearing errors vs azimuth

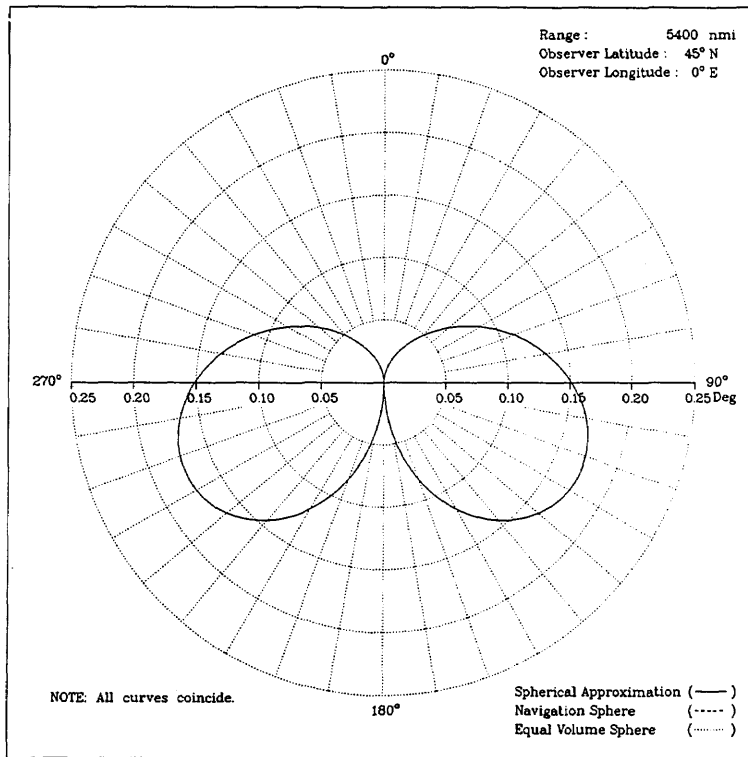


Fig. E11 — Spherical Earth bearing errors vs azimuth

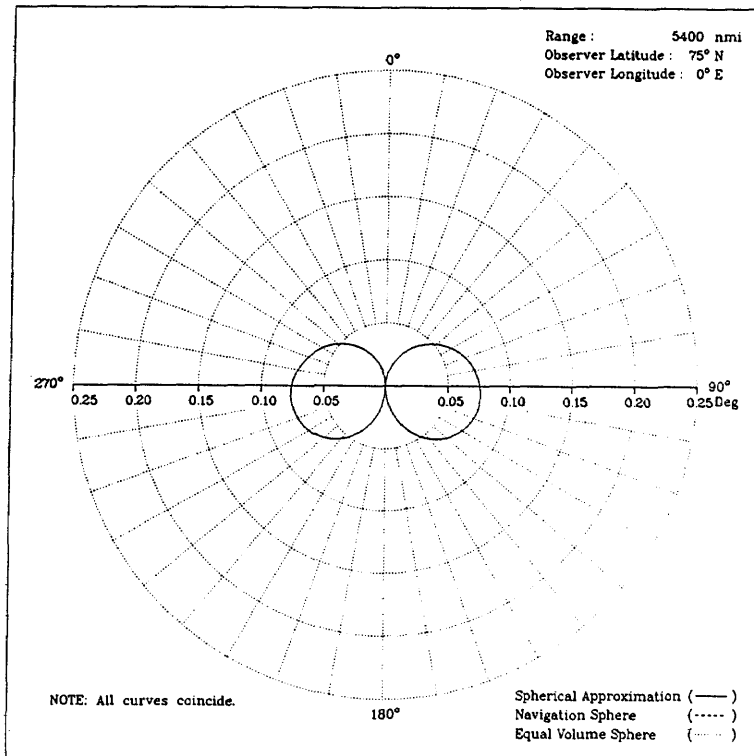


Fig. E12 — Spherical Earth bearing errors vs azimuth

PICH AND LEROY

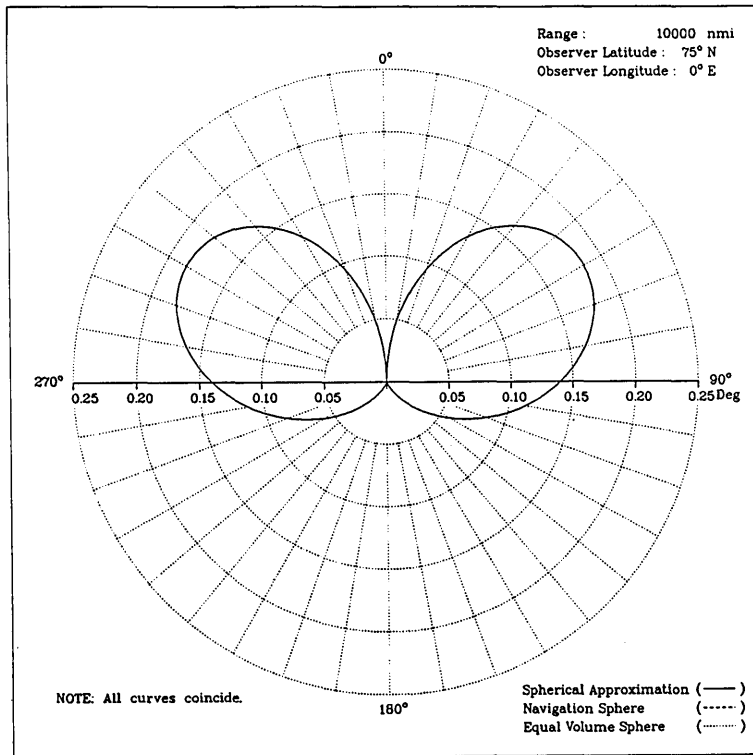


Fig. E13 — Spherical Earth bearing errors vs azimuth

## **Appendix F**

### **COMPARISON OF FLAT EARTH MODELS TO SPHERICAL APPROXIMATION MODEL**

Figure F1 shows the 0.5-nmi maximal error also shown in Fig. D1 at a range of 100 nmi with the observer at the equator. Similar calculations are also performed by using the Spherical Approximation model and placed on the same graph in Fig. F1. For these close-in distances at the equator, the flat Earth approximations tend to yield a slightly better approximation to the WGS-84 ellipsoid than does the Spherical Approximation. For example, we can perform range calculations as far out as 200 nmi before incurring a 1-nmi mile error with either flat Earth model whereas the Spherical Approximation would incur this error at approximately 175 nmi. However, these results are only true at the equator. Figures F2 through F7 provide similar plots at different latitudes on an equal maximum range error scale for ease of comparison. From these plots it is clear that on the average (that is, over many latitudes) the Spherical Approximation outperforms the flat Earth models. At 85°N the flat Earth models deteriorate rapidly.

To better understand the characteristics of the Spherical Approximation model at longer distances, we performed tests at 0°, 15°, 30°, 45°, 60°, 75°, and 90° north observer latitudes. Ranges from 10 to 5400 nmi were selected, and plots of the maximum error from each range vs distance from the observer were drawn. Figures F8 through F14 show the resultant plots. When the observer is on the equator, as in Fig. F8, the maximum error is 10.5 nmi, occurring at a range of 2900 nmi. The maximum error, 21 nmi, is shown in Fig. F11 with an observer latitude of 45°N. This point occurs at a range of 5400 nmi from the observer. As the observer moves farther north in latitude (Figs. F12 through F14), the error decreases.

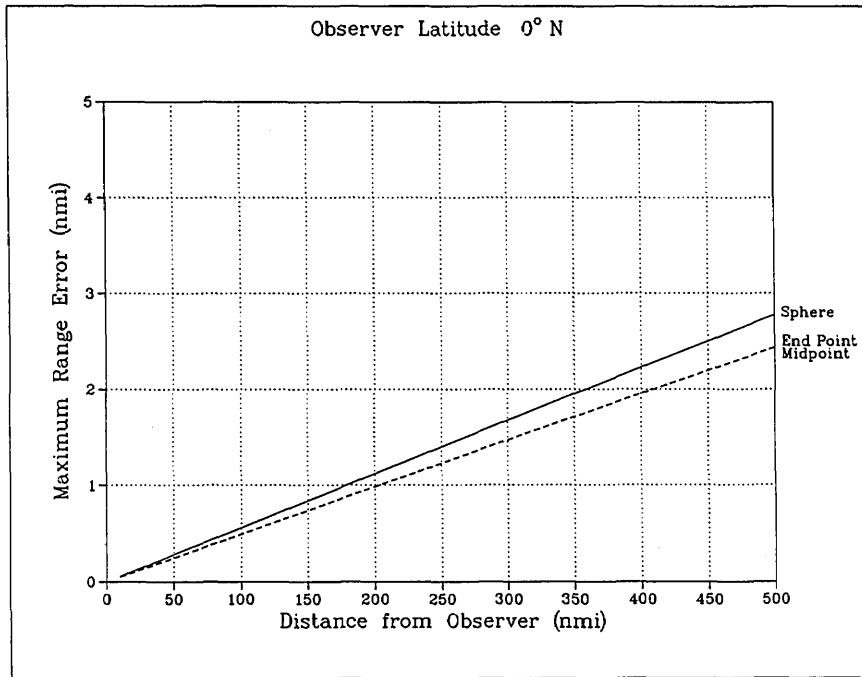


Fig. F1 — Surface range errors vs surface range

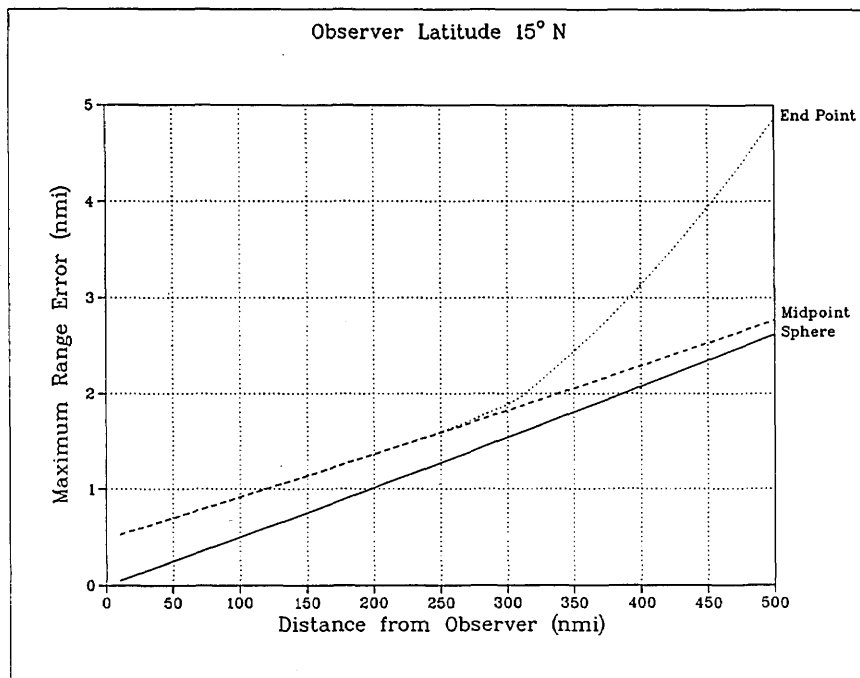


Fig. F2 — Surface range errors vs surface range

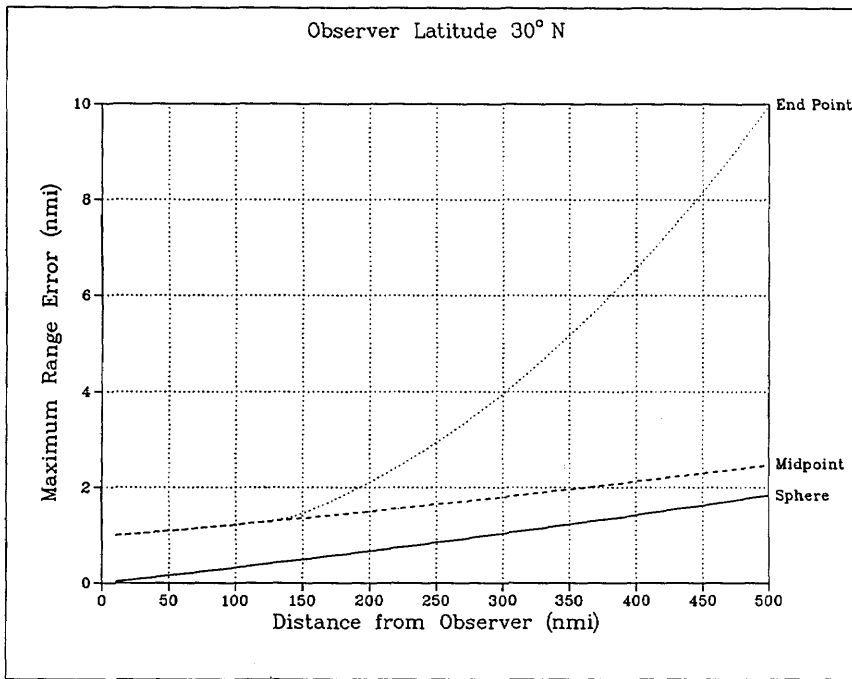


Fig. F3 — Surface range errors vs surface range

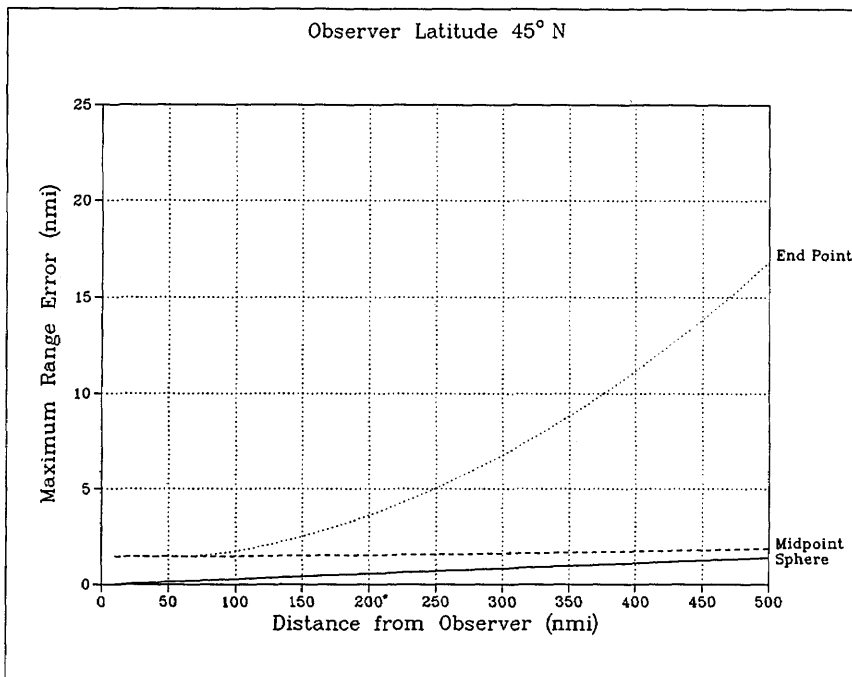


Fig. F4 — Surface range errors vs surface range

PICH AND LEROY

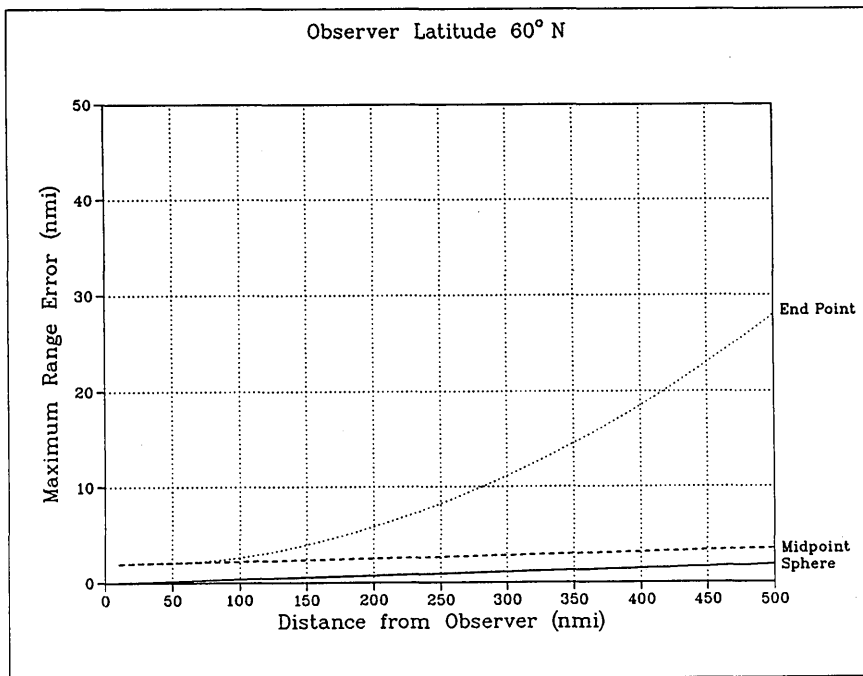


Fig. F5 — Surface range errors vs surface range

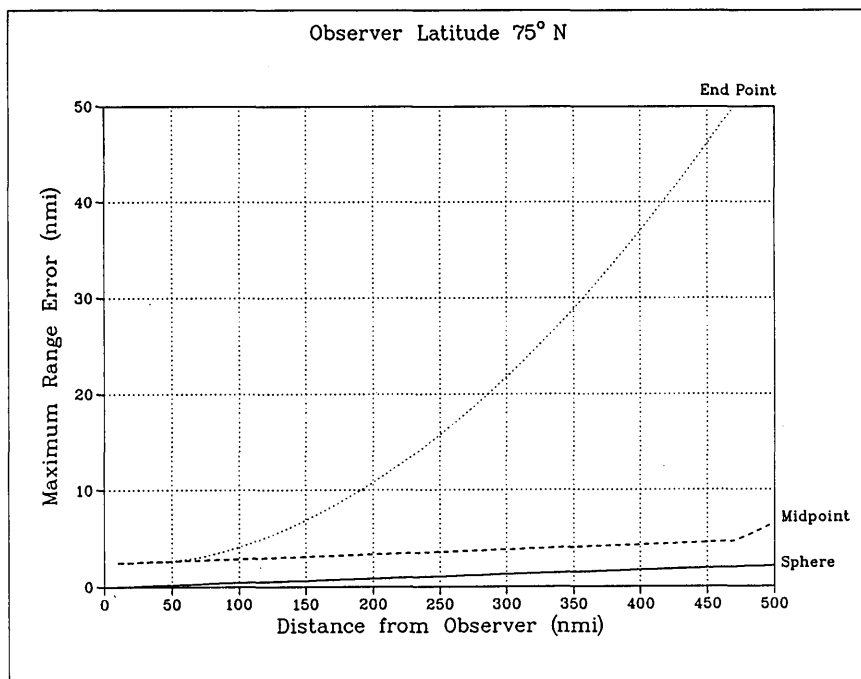


Fig. F6 — Surface range errors vs surface range

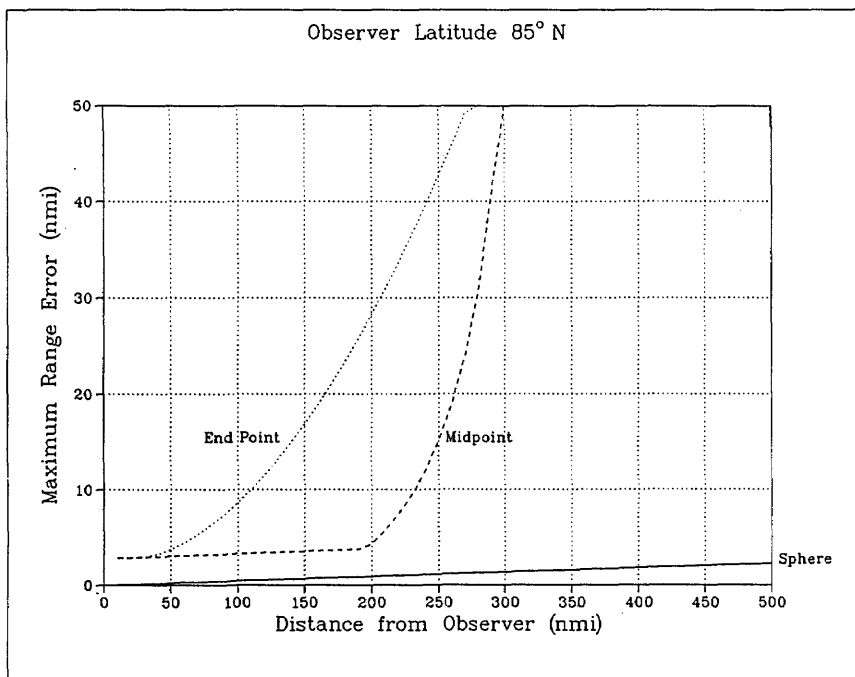


Fig. F7 — Surface range errors vs surface range

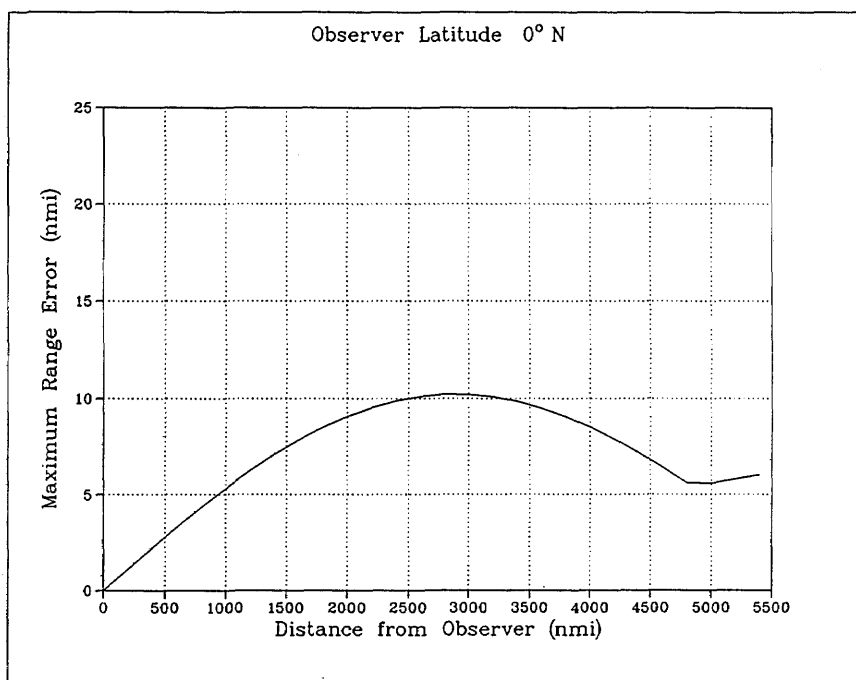


Fig. F8 — Spherical Approximation surface range errors vs surface range

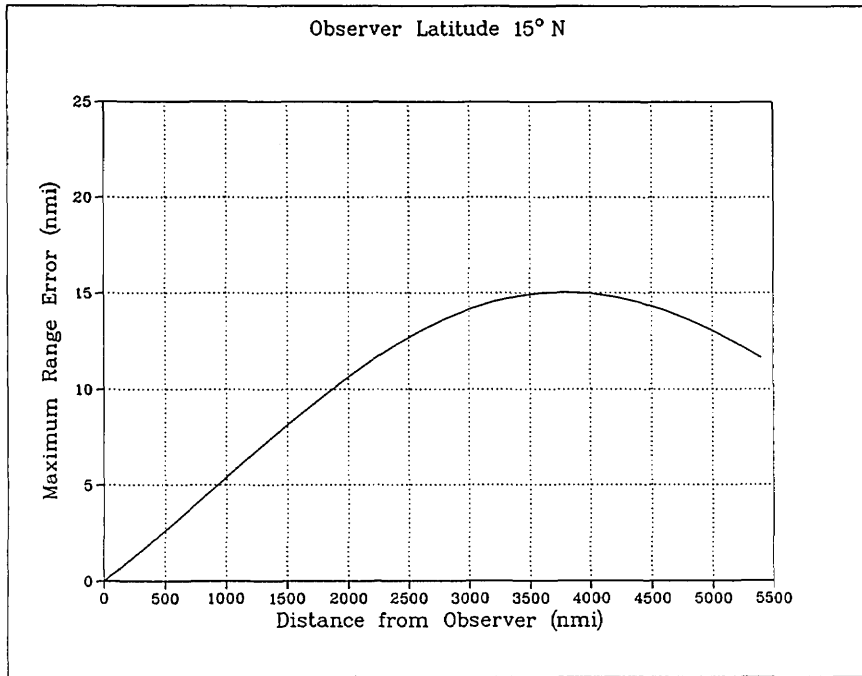


Fig. F9 — Spherical Approximation surface range errors vs surface range

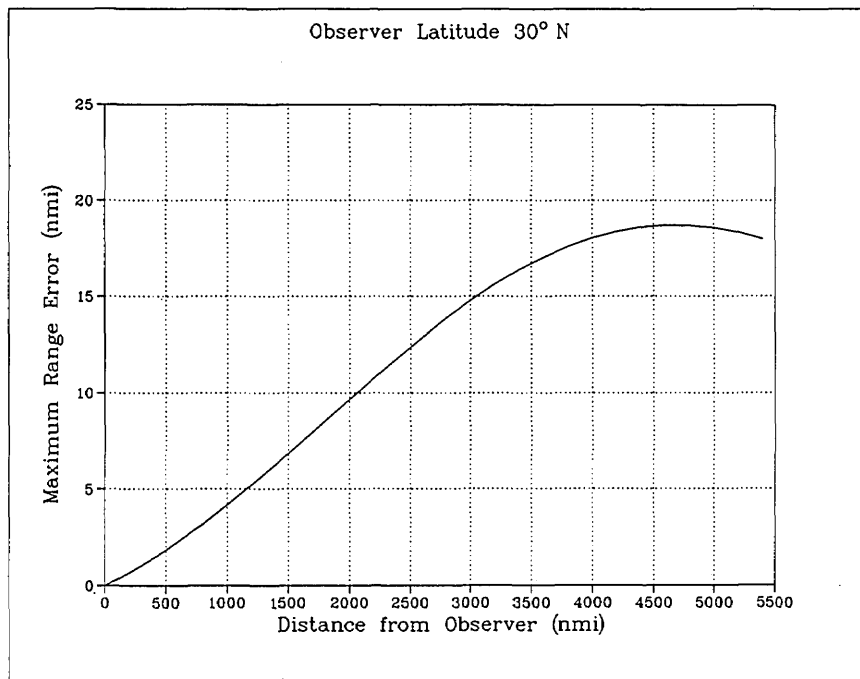


Fig. F10 — Spherical Approximation surface range errors vs surface range

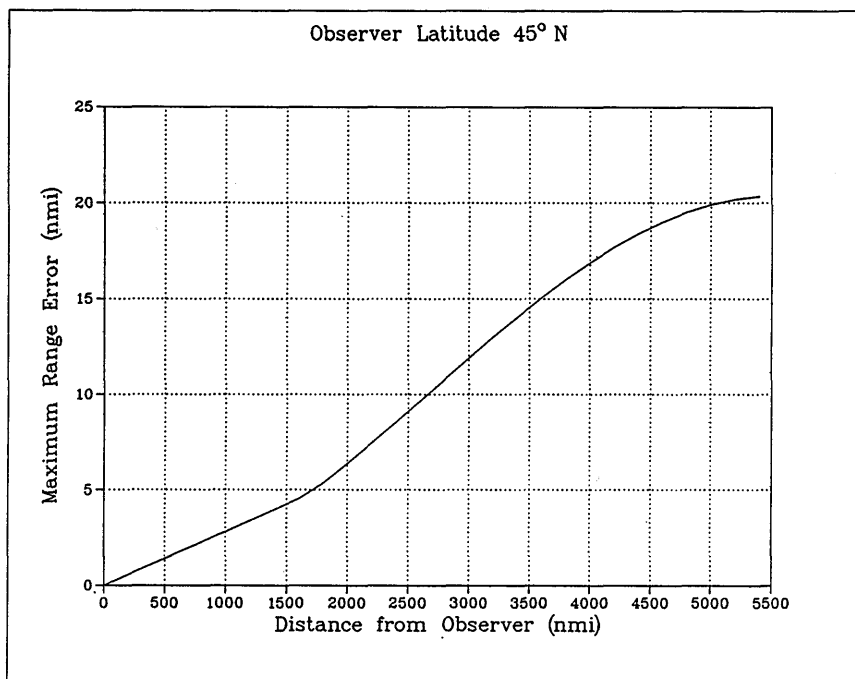


Fig. F11 — Spherical Approximation surface range errors vs surface range

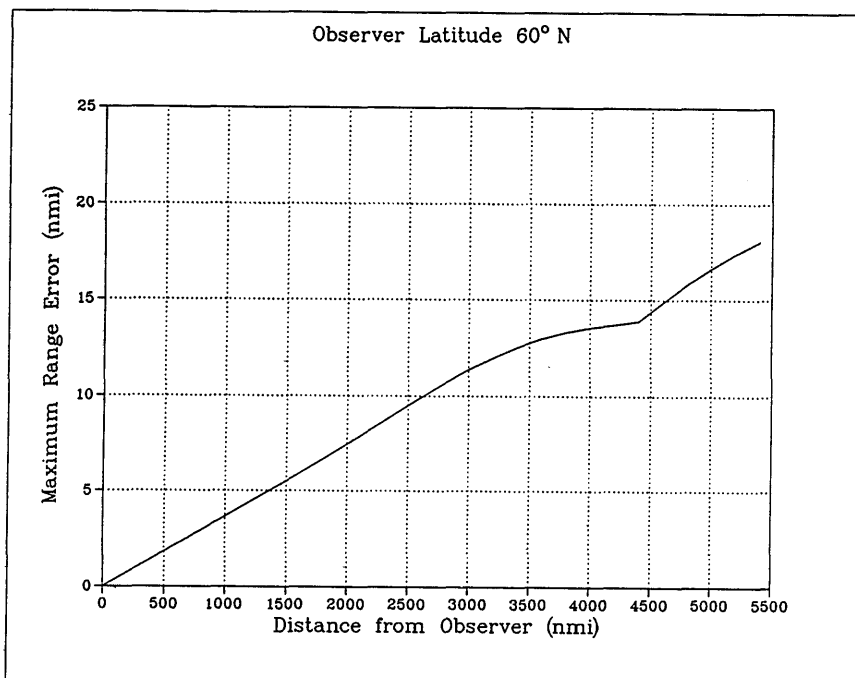


Fig. F12 — Spherical Approximation surface range errors vs surface range

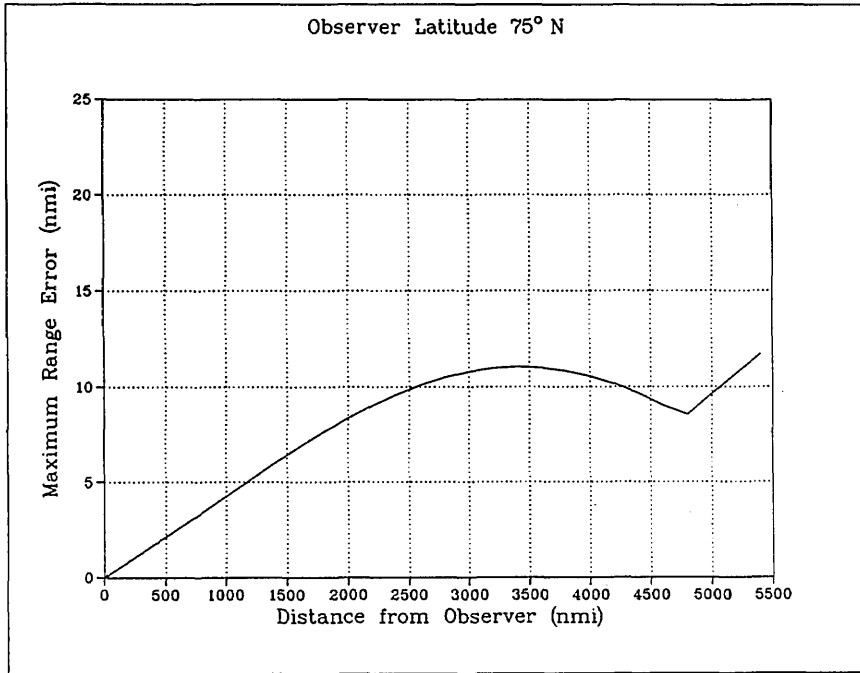


Fig. F13 — Spherical Approximation surface range errors vs surface range

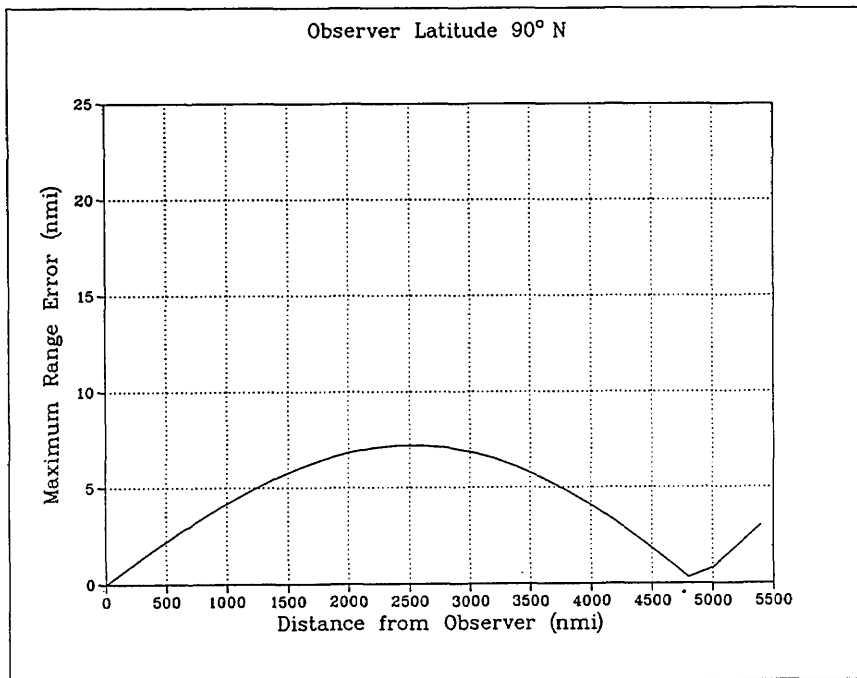


Fig. F14 — Spherical Approximation surface range errors vs surface range